HEAD ROLL INFLUENCES ON MULTI-SENSORY INTEGRATION FOR PERCEPTION AND ACTION

by

Jessica Katherine Burns

A thesis submitted to the Centre for Neuroscience Studies

In conformity with the requirements for

the degree of Master of Science

Queen's University

Kingston, Ontario, Canada

(September, 2010)

Abstract

The representation of ourselves and our environment is based on the combination of information from multiple sensory systems. Each sensory modality is represented within a different frame of reference, in other words each sensory system uses a different code to represent the same properties of the environment (ex. visual stimuli in an eye-centered frame of reference; hand position would be shoulder-centered). Combing this information into a singular coordinate frame is complex. For instance, the eye and shoulder have different centers of rotation, therefore any changes in eye position or body posture will affect the relationship between them. What is still unknown is how the brain integrates these different sources of information into an internal representation, and what effect extra-retinal signals can have on this process. This thesis was designed to investigate the effect of head roll on action and perception. In Experiment 1, we wanted to determine how the integration of vision and proprioception for action was affected by changes in head roll. To investigate this question subjects performed a reaching task at three different head roll positions, where they would experience conflicts between their viewed and actual hand position. In Experiment 2, we examined the influence of head roll on sensory perception. To explore this idea subjects performed a task where they needed to judge the position of their unseen index fingertip relative to a visual target. Our findings reveal that eccentric head roll conditions influence both action and perception – revealed by an increase in movement variability and a decreased ability to discriminate the position of the unseen fingertip relative to visual targets. In summary, we have discovered that introducing eccentric head roll positions affects the perception of ourselves within the environment and the way that we integrate sensory information.

Co-Authorship

The research described in this thesis was conducted by Jessica Burns under the supervision of Dr. Gunnar Blohm. Jessica Burns conducted the testing and analysis of the data described in Chapters 3and 4, and wrote the first draft of each chapter within this thesis. Joseph Nashed assisted with the analysis of data that is represented in Chapter 4. Dr. Gunnar Blohm was solely responsible for any mathematical modeling that is described within this thesis.

Acknowledgements

First and foremost I would like to thank my supervisor Gunnar Blohm. Your patience, guidance and encouragement throughout this processes has helped me to become a better researcher. I would also like to express my appreciation to Joseph Nashed who was largely involved in my second research project. Thank you for always taking the time to help me when I was stuck on a problem. I would like to thank both Randy Flanagan and Stephen Scott for letting me use their labs to complete both of my projects, this thesis would not have happened without their generosity. Thank you to Martin York and Justin Cadwell who helped to get my first project going; I really appreciate all of your time and hard work. To Justin Peterson, you were the one to get my second project going in lightening speed, so thank you for that.

Lucy Russo-Smith and Kelly Moore, where do I even begin to list all of the things you have both done for me. Thank you for always taking the time to help me with my numerous requests and being there for me when I needed mind break. Both of you helped me keep my sanity, and that deserves a huge thank you.

To all of my friends and family, you have been a tremendous support throughout this process, your encouragement and kindness had been remarkable. To Mom, Dad and Emily; I cannot fully express how your love and support throughout this step of my life has helped in my success. You have constantly encouraged me to follow my dreams and I cannot thank you enough. I would like to finish off by thanking Neil for his love, support and encouraging me to be the best I can be.

Table of Contents

List of Figures

List of Abbreviations and Symbols

ANOVA	Analysis of variance
cm	centimeters
CNS	Central nervous system
CCW	Counter clockwise
CW	Clockwise
EOG	Electrooculography
H	Head roll
IHP	Initial hand position
L	Length
LGN	Lateral geniculate nucleus
M1	Primary motor cortex
MLE	Maximum-likelihood estimation
MSTd	Medial superior temporal area
mm	Millimeters
mV	Millivolts
OCR	Ocular counterroll
P	Proprioception
PMd	Dorsal premotor cortex
PMv	Ventral premotor cortex
PPC	Posterior parietal cortex
SD	Standard Deviation
S.E.M.	Standard error of mean
T	Transformation
V	Vision
V1	Primary visual cortex
VOR	Vestibular ocular reflex
VSP	Visual start position
VT	Visual target
α	Weight
β	Head roll compensation gain
Δx	Desired movement vector
$\Delta\theta$	Change in joint angles
θ_1	Arm deviation from straight ahead
θ_2	Upper arm elevation
σ_H^2	Head-roll-dependant vairance
σ_P^2	Proprioceptive Variance
σ_V^2	Visual Variance
Σ_H	Constant transformation noise
$\neq$	Not equal
*	Significant

Chapter 1

Introduction

Every day we seamlessly interact with our environment rarely considering the complex processes that enable these interactions. Regardless of how simple the task, whether it be writing on paper, pouring milk on cereal, or exchanging a high five, multiple pieces of sensory information regarding ourselves and our surroundings must be incorporated to achieve success at any task. This process is known as multi-sensory integration, and involves combining sensory information from multiple modalities to form an accurate representation about specific objects or events (Ernst and Bulthoff, 2004).

Sometimes this information is congruent between the sensory modalities and sometimes it’s not., The brain needs to assess the reliability of the sensory signals for each sensory modality and weight that information accordingly (Kording and Wolpert, 2006; Ernst and Banks, 2002). The reliability of these sensory signals can be calculated based on previous experience or determined on-line depending on the context of the environment (Ernst and Bulthoff, 2004).

Any uncertainty associated with sensory signals can be attributed to noise within the system (Fasisal et al., 2008). For example, during a visually-guided movement being able to see the target clearly, attributes greatly to the movement accuracy. Conversely, if target visibility is degraded by dimming the lights, then the visual signals associated with target location would be subjected to a certain amount of noise. Any noise that is present will create a level of uncertainty about the sensory signals, and therefore affect the perception of the sensory information, as well as the generation of motor responses. The relative uncertainty associated with any sensory signal will affect the weight given to that information during integration (Fasisal et al., 2008).

For information to be integrated, the acquired sensory signals need to be encoded within same coordinates (Buneo and Andersen, 2006; Blohm, et al. 2009; Knudsen et al., 1987; Soechting and Flanders, 1992). The conversion of one signal type to another is a process known as a reference frame transformation. Once signals are represented in the same coordinates, they can be compared and weighted, to create the most accurate representation of the specific object or event.

The specific details about signal transformations are still up for debate. The purpose of this thesis was to determine if simply altering head orientation can influence self perception or the way that sensory information is weighted and integrated. Introducing head roll into both perceptual and movement tasks is a way to induce changes in body geometry, thus creating a certain level of uncertainty within the system. In other words, head roll is an extra-retinal signal that is simply used to push noise into the system. What our subsequent experiments' test is in what ways this noise affects the sensory integration processes.

Chapter 2

Literature Review

2.1 An Overview

Everyday our brains incorporate incoming information from various sensory modalities to reconstruct our external environment. This process is often referred to as multi-sensory integration and our motor system relies on it in order to effectively act on or within our surroundings. For instance, when reaching for a pen on our desk, we map its spatial location relative the position of our hand. These differences in location are compared so that our system can formulate a motor plan. The integration of the visual and proprioceptive information is critical in order for us to successfully complete the task. In the two studies that follow this review, both visual and proprioceptive sensory systems have been used to study the effect of head roll on multi-sensory integration. Having an overview of the components of vision and proprioception will facilitate a better understanding of how each of these systems are involved in the integration process. Next, this review dives into a section on multi-sensory integration itself, describing how noise affects the system and the details involved with reference frame transformations. From there, important neurophysiological and computational sensory integration theories are summarized. To study the effect of head roll on multi-sensory integration, we conducted a reaching experiment. This review finishes off by describing how target and hand positions are calculated to create a movement plan that is then transformed into action.

2.2 The Visual System

2.2.1 The Importance of Vision in Multi-Sensory Integration

The visual system is extraordinary in its ability to transmit information about the external world into a signal that our central nervous system uses to identify objects, determine distances and gage movements. Thereby, vision is vital for our body to navigate through space, and its accuracy in part, is what gives us precision in our movements. It is this sensory modality that experience has taught us to be the most resourceful and therefore the one we rely most heavily upon. The first investigator to document visual dominance was J. J. Gibson in 1933. The experiment consisted of subjects wearing prism glasses that made straight lines appear curved. As subjects watched their hand run along a straight edged object, they reported feeling the object as curved. The strength of visual over kinesthetic perception was so strong that subjects were unable to dissociate them (Gibson, 1933). Since this experiment, many researchers have attempted to determine our reliance on visual information and its relative weight compared to proprioceptive inputs.

2.2.2 Neural Substrates for the Processing of Visual Information

In order to create an integrated perception of the environment, visual information needs to travel through various structures and pathways (for review see Purves et al., 2008). It all begins with visual information passing through the retina. From there this information is sent into the central nervous system via the optic nerve. The optic nerve takes this information from the retina and carries it to the optic chiasm where the nerve fibers follow one of two fates; continue travelling along the same side of the brain or cross over to the other side. These two fates create two groups of fibers, each becoming an optic tract that carries information from both eyes. The main target of these nerve fibers is the dorsal lateral geniculate nucleus (LGN), located in the thalamus. The LGN relays visual signals through optic radiation to the primary visual cortex (V1) (Purves et al., 2008). Different regions of the retina are represented in different regions of V1, each contributing to synthesis of a visual representation. The processing of visual stimuli does not stop at the primary visual cortex; it carries on into two primary pathways. Travelling into the parietal lobe, the dorsal stream is responsible for mapping spatial locations and analyzing motion, both of which are essential for reaching movements. The ventral pathway extends into the temporal lobe and is used for object recognition, allowing elements in external space to be understood.

2.2.3 Visual Stabilization During Head Movements

It is critical to keep visual input as precise as possible. Therefore the central nervous system developed mechanisms to stabilize gaze during static and synamic head movements. The vestibular ocular reflex (VOR) is a mechanism that allows visual fixation to be maintained regardless of head movements (Seidman and Leigh, 1989). The vestibular system participates in determining the degree, direction and speed of head movement, and the eyes respond by counteracting this movement (Seidman and Leigh, 1989). For example, if the head is turned to the right, the eyes would move left with the same magnitude and velocity, but in the opposite direction. The degree to which the eyes move, divided by how much the head was moved is known as gain (Crawford and Vilis, 1991). If the eye and head move with the same magnitude, but in opposite directions, the gain of VOR should be close to one.

Vertical and horizontal head rotations usually have a gain that is close to one, whereas when the head is tilted about the nasal-occipital axis (roll or torsional rotation) the gain is typically less than 0.7 (Seidman et al., 1995). Although there is no clear reason as to why these differences occur, some suggest that vertical and horizontal head movements tend to displace the images away from the fovea much more than head roll movements do (Leigh and Zee, 2006). Perhaps the differences in gain are due to the fact that head rotations in roll do not cause the image to slip when the line of sight is parallel to the axis of head rotation (Seidman et al., 1995).

Researchers have also found dramatic differences in compensatory eye movements between dynamic and static head rotations. The vestibular ocular reflex compensates for dynamic head roll, whereas ocular counterroll responds to static head roll positions. When the head is maintained in a stationary rolled position, ocular counterroll (OCR) only compensates for about 10% of the total head rotation (Collewijn et al., 1985). Researchers attribute the differences between VOR and OCR to the different signals sent from the vestibular system. Dynamic head rotations stimulate both the semicircular canals and the otolith organs, where the information about angular acceleration is sent along a pathway eventually activating the motoneurons of the eye muscles (Angelaki et al., 1999; Fischer, 1927, as cited in Collewijn et al. 1985; Markham, 1989). Conversely, when the head is statically maintained in a rolled position, gravitational forces stimulate the otolith organs of the vestibular system, which through a series of events result in an occular counterrroll (Miller et al. 1968; Fischer, 1927, as cited in Collewijn et al.1985; Markham, 1989). The differences in gain between static and dynamic head roll could be attributed to the decrease effectiveness of the otolith organs as the angle of head roll increases (Lechner-Steineitner, 1978; Schone and Udo de Haes, 1968). In order to create an accurate representation of the external environment, the brain needs to account for ocular torsion and the differences that occur between dynamic and static head roll.

2.3 The Role of Proprioception in Perception and Action

Proprioception is the knowledge of our body's orientation, provided by mechanoreceptors in the muscles, tendons and joints (Goodwin et al., 1972; Proske, 2005; Binder et al., 1977; Clark and Burgess, 1975). It allows individuals to gain knowledge about body position within the external environment to allow successful interaction. Proprioception plays a role not only in planning movements but controlling them as well. In 1979, Polit and Bizzi conducted a pointing study with deafferented monkeys. Before afferent information of the arm was eliminated, the monkeys were trained on the pointing task until they were proficient. They found that pre and post surgery monkeys were able to successfully complete reaching movements to the final target. The results were unclear as to whether the monkeys were planning new movements or just recalling them (Polit and Bizzi, 1979). They discovered that when the deafferented monkeys' arms were repositioned relative to their bodies, they could no longer perform the movements accurately. Conversely, when the arms were repositioned prior to surgery, they were able to successfully compensate for these changes (Polit and Bizzi, 1979). This study demonstrates that proprioceptive information is needed to accurately plan movements, in particular when compensating for changes in body positions.

In addition to motor planning, proprioception is also important for motor control. During movement, proprioceptors provide sensory feedback that can be used to correct actions (Gandevia and Burke, 1992). If no online corrective adjustments can be made, due to time constraints, the sensory feedback can be used in motor learning to correct future movement errors (Kawato et al. 1987; Diedrichsen et al. 2007).

2.3.1 The Importance of Muscle Spindles

Muscles spindles are located within the skeletal muscles, and play a significant role in supplying detailed knowledge about the state of muscles. Goodwin and colleagues (1972) were the first to suggest that discharge from muscle spindles can contribute to proprioception. They induced a proprioceptive illusion using a muscle vibration technique. When the biceps muscle was vibrated, subjects perceived an extension in the elbow, even though the arm remained still (Goodwin et al. 1972). This illusion occurs because the vibration excites the muscle spindles in a similar manner to when they are actually being stretched (Burke et al., 1976; Goodwin et al. 1972).

Muscle spindles are composed of 2-10 intrafusal muscle fibers (Bergman et al., 1999). The central part of intrafusal muscle fibers are encircled by two types of sensory nerve endings, primary and secondary (Purves et al. 2008; Hulliger, 1984). Sensitive to dynamic stretch, the primary nerve endings transmit information about velocity and direction of movement, whereas information pertaining to the static position of the muscles is provided by the secondary endings (Purves et al. 2008, Hulliger,1984). When the muscle fibers are stretched, so are the intrafusal muscle fibers. The primary and secondary nerve endings surrounding the intrafusal muscles fibers become physically deformed. These deformations cause signals to be sent to the brain regarding the changes in muscle length (Purves et al. 2008; Hulliger, 1984).

2.3.2 Other Sources of Kinesthetic Information

Golgi tendon organs are an additional key component of proprioception, because they are responsible for gauging muscle tension and force (Schoultz and Swett, 1973, Armstrong, McNair and Taylor, 2008). Joint receptors are another source of proprioceptive information, however playing a more supportive role in determining position sense. They help to detect extreme movements (end of joint range of motion), thereby protecting the joint from injury. (Proske et al., 1988; Clarke and Burgess, 1975). Cutaneous receptors are another mechanism that relay information about the position of nearby joints (Gandevia and McCloskey, 1976; Edin and Abbs, 1991; Collins et al. 2005). Alone, cutaneous receptors are not extremely effective; however when activated simultaneously with muscle spindle receptors the perception of movement is increased compared to when muscle spindles or cutaneous receptors are activated alone (Collins et al. 2005).

Efference copies are another mechanism used in determining our position sense. Efferent copies of motor signals are compared with the afferent signals that are received from the proprioceptors (Scott, 2004; Bridgeman, 1995). In terms of a reaching movement, the estimate of the current positions of the hand and joint angles are compared to the efference copy, which is a plan of where the hand would like to move (Scott, 2004; Wolpert et al. 1995; Kawato et al. 1987). In essence, the system can use this information to update motor commands and optimize performance even in the presence of noise (Scott, 2004).

2.3.3 Determining Head Orientation

There are a number of sensory components that play a part in determining head orientation. Similarly to the rest of the body, the muscle spindles in the neck are the primary proprioceptive contributors to position sense. Anatomical studies have found that the deep cervical neck muscles contain the highest densities of muscle spindles (Peck et al., 1984; Liu et al. 2003). The information obtained from muscle spindles is combined with supplementary information from cutaneous and joint receptors. Together this information provides the central nervous system with a proprioceptive estimate of head position.

In addition to this, the vestibular system provides important sensory information about the orientation and movement of our head in space. The vestibular system is comprised of two types of sensory organs, the semicircular canals and the otolith organs (Purves, 2008). There are three semicircular canals, each of which responds to different angular accelerations of the body or head (Purves et al. 2008; Baloh and Honrubia, 2001; Bensen, 1982). The second sensory component of the vestibular system is the otolith organs; they detect changes in linear accelerations and static head positions (Purves et al. 2008; Baloh and Honrubia, 2001; Bensen, 1982). Sensory information from the vestibular system is combined with the inputs from the visual system and neck proprioceptors and takes part in an integrative approach in accurately determining head position sense (Purves et al. 2008). However, each of these sensory components is represented in different frames of reference, in other words visual and vestibular information represent the signals with different viewpoints. In order for their information to be combined, it needs to be transformed into a common reference frame, or a comparable representation (Crawford et al. 2004; Blohm and Crawford, 2007).

2.4 Multi-Sensory Integration

Combining sensory signals is the most effective way in obtaining the most accurate and reliable representation of our environment (Ernst and Bulthoff, 2004). Multi-sensory integration refers to the convergence of sensory inputs all representing the same aspect of the environment (Ernst and Bulthoff, 2004). The actual process of multi-sensory integration is very complex, and the precise details are still unknown. Behavioural, computational and neurophysiological studies have each contributed to the theories that have been previously put forth. Yet, not one theory can fully describe or account for both the behavioural and neurophysiological observations. Determining how noise, reference frame transformations, and weighting of sensory information all occur in the brain are questions that still do not have well defined answers.

2.4.1 The Effects of Neural Noise

Sensory information enters our system as some form of energy, and is then converted into a mechanical or chemical signal. For example, as our heads tilt away from an upright position, the semicircular canals generate mechanical signals that are then converted into electrical ones (Fasisal et al., 2008). Each of these signals are intrinsically noisy, and as a result this noise will create a level of uncertainty about the sensory information. This noise in turn will affect the perception of the sensory conditions, as well as the generation of motor responses (Faisal et al. 2008; van Beers et al., 2002). During movement planning the inherent goal is to minimize the variance of the effector's final position (Harris and Wolpert, 1998). Any noise in the movement planning stage will cause the trajectories to deviate from the desired path (Harris and Wolpert, 1998). For instance, if there is noise associated with the sensory information about a target's position, it will cause uncertainty about its true location, then this leads to errors or variability in the motor commands (van Beers et al., 2002). With goal directed movements, neural noise is not only present during target localization and motor planning, but largely during movement execution as well (van Beers et al., 2002; van Beers et al., 2004). Any noise that is present during movement planning and execution will lead to variability in our movements, resulting in decreased accuracy and precision (van Beers et al., 2002).

2.4.2 Reference Frame Transformations

The concept of multi-sensory integration is taking different forms of sensory information that are representative of the same object or event and combining them to create the most accurate description or account (Ernst and Bulthoff, 2004). One problem is that different forms of sensory information are coded in different frames of reference, and in order for the data to be combined it needs to be coded in the same coordinates (Crawford, et al., 2004; Blohm and Crawford, 2007; Knudsen et al, 1987). This conversion process is known as a reference frame transformation.

A key example of a reference frame transformation occurs during movement planning. When creating a plan to move towards a visual target, knowledge about the target position, as well as the hand location needs to be integrated (Henriques et al. 2002; Rossetti et al. 1995). Both the target and hand position are represented in visual coordinates, but the hand position is also represented in proprioceptive coordinates.

Visual coordinates refer to the location of objects being mapped in relation to the retina or center of the eye. Combining visual and proprioceptive information about hand position has shown to improve task performance, when compared to tasks with only one type of sensory signal (van Beers et al. 1999; Wolpert, 2007). Proprioceptive signals about hand location and thus limb configuration, are used to help plan how the joint angles need to change in order to successfully reach the target (Sainburg et al. 1995; Sober and Sabes, 2005). Movements to visual targets are believed to be planned in visual coordinates, therefore the proprioceptive information needs to be transformed into visual coordinates in order for all of the information to be combined and used for reach planning. (Buneo et al, 2002 ;Sainburg et al. 2003; Sober and Sabes, 2005). Not only do transformations occur during movement planning, but in order for that plan to take effect, the movement plan information that is represented in a visual coordinate frame, needs to be transformed into a proprioceptive or shoulder-centered frame of reference (Desmurget et al. 1998 ; Sober and Sabes, 2005). A shoulder-centered frame of reference refers is a term used to describe the position of the hand with respect to the shoulder.

Although reference frame transformations are necessary for the integration of different sensory information, this transformation can incur a cost and translate into errors in movement planning, and impairments in motor performance (Sober and Sabes, 2005; Soechting and Flanders, 1989; Sarlegna et al., 2009). These errors could be the result of misaligned visual and proprioceptive coordinate frames, or because of the noise added into the transformed signal itself (Sober and Sabes, 2005; Schlicht and Schrater, 2007; Soechting and Flanders, 1989)

2.4.3 Sensory Integration Theories

Multiple sensory systems provide information about the environment, helping us to guide our actions within it. With more than one sensory system providing the same details, these redundant signals are integrated to create the most reliable estimate (Helbig and Ernst, 2008).

2.4.3.1 Neurophysiology

Sensory signals enter the nervous system through their respective pathways, but in order for these signals to be integrated, they need to have access to the same neurons; this will allow these signals to be represented in the same units (Stein and Meredith, 1993). The convergence of different sensory signals on to individual cells happens in many areas of the nervous system, but the superior colliculus (SC) contains a rich source of multi-sensory neurons, allowing researchers to more effectively study their properties. What is more fascinating than the multisensory neurons themselves is that SC is arranged so that the spatial maps of visual, auditory, and somaotosensory maps overlap one another (Stein and Meredith, 1993; Meredith and Stein, 1986). Therefore stimuli originating from the same location in sensory space are integrated in the same area of the superior colliculus.

The information gathered from studying the superior colliculus can give us insight into the processes that may be occurring in other cortical areas. Understanding how neurons integrate the information optimally is another question. Ma and colleagues created neural networks to explain how neuronal circuits may perform multi-sensory integration (2006). They suggest that different sensory information is coded by separate populations of neurons, which could be combined by simply adding both representations together (Ma et al., 2006). This theory inspired Gu and colleagues to see if multimodal neurons combine different sensory input in this way (2007). They studied neurons in the dorsal medial superior temporal area (MSTd) during a heading discrimination task, where subjects determined the direction of self motion. The role of MSTd has been shown to be involved in heading perception in terms of visual motion; however, the idea that vestibular signals may be involved as well was not yet known (Tanaka and Saito, 1989; Duffy and Wurtz, 1991). Gu and colleagues tested to see if non-visual (vestibular) responses in MSTd neurons, were correlated with heading perception (2007). Their results supported this hypothesis, as MSTd is not singularly a visual area, but receives contributions of non-visual cues as well (Gu et al. 2007). Further research by Gu et al. found that visual and vestibular cues are combined linearly in area MSTd (Gu et al. 2007). This study provides neurophysiological evidence of the neural mechanism involved in multi-sensory integration. However, these physiological studies have not addressed the fact that sensory modalities are represented in different coding schemes, and thus a simple linear combination is not favorable without reference frame transformations. As a result, computational approaches have set out to explain the uncertainties that neurophysiological studies have not yet addressed.

2.4.3.2 Computational Neuroscience

As our nervous system receives a plethora of incoming signals from different modalities, it needs to determine what information is important and relative prior to sensory weighting and integration (Ghahramani et al., 1997). There are a number of theoretical views pertaining to how information from different sensory modalities is integrated. One belief is that the modality that is the most appropriate for a given situation will dominate; in spatial tasks for example, vision would dominate over audition. This theory is referred to as the modality appropriate hypothesis (Welsh and Warren, 1986 as cited in Ernst and Bulthoff, 2004). By contrast, if there is a conflict between two sensory inputs, one of the senses may simply dominate, while the others are ignored, in a competitive integration approach (Ghahramani et al. 1997). The problem with both of these theories is that in each case the nervous system tends to rely mostly on one sensory modality. Every estimate that is created by the sensory system is corrupted by noise, and as a result the uncertainty associated with the estimates created by a single modality cannot be reduced (Ernst and Banks, 2002). Making use of all available information is optimal because it maximizes the probability of creating the most accurate estimate (Ernst and Banks, 2002). As a result of a constantly changing environment, the reliability of individual sensory modalities can vary considerably (Deneve and Pouget, 2004). The benefit of integrating sensory information is simply to reduce the variability associated with individual incoming cues (Ernst and Bulthoff, 2004; Helbig and Ernst, 2008).

Perceptual judgments allow us to determine the variances associated with different cues, and these uncertainties determine how the cues should be optimally weighted during sensory integration (Knill and Pouget, 2004). The weighting of information simply refers to contribution it will give to the final estimate. Bayesian statistics are commonly used to help define how sensory information from two modalities can be merged into one (Kording and Wolpert, 2006). In order to combine the cues, each needs to be weighted according to the uncertainty and noise associated with them

(Kording and Wolpert, 2006). To minimize the variance in the final estimate, the maximum-likelihood estimation (MLE) is used (Ernst and Banks, 2002). The MLE rule states that the combined estimates should have a lower variability compared to the individual modality estimates (Ernst and Banks, 2002).

If perhaps there is uncertainty with a particular sensory signal in a given environmental condition, incorporating prior beliefs about the possibilities that could be occurring for this situation can help to resolve these ambiguities. For example, if you are able to see only the shadow of someone you know, but not their face, you would probably be able to tell who they were based on your prior knowledge of their stature. Bayesian theory takes into account our prior beliefs (prior probability) and determines how it should be combined with the new information (likelihood) to obtain the most reliable estimate (Kording and Wolpert, 2006)..

Having a theory that explains how multiple sensory cues are optimally combined is only one part of multi-sensory integration, knowing how cues from different frames of reference are integrated is another problem. For example in reach planning, sensory information about hand location is represented in both proprioceptive and visual coordinates, but this information cannot be integrated until it is represented by the same code. There are a number of theoretical models that try and explain how the brain combines signals that are coded differently. In terms of coordinate transformations that occur during visually guided reaching, one proposed method that was generally accepted suggested that visual target positions were transformed into body centered coordinates, where they were compared with the body centered location of the hand (McIntyre et al., 1997,1998). After this study, researchers recording from the posterior parietal cortex reported that target locations are coded with respect to the eye and the hand (Buneo et al. 2002). If visual information about the hand was not available, then proprioceptive information obtained would be transformed in to gaze centered coordinates (Buneo et al. 2002). This information could be used to create a movement vector in visual coordinates that could later be transformed into a shoulder centered frame of reference for movement (Buneo et al. 2002; Crawford et al., 2004). By contrast to these proposed theories, Sober and Sabes suggest that vision and proprioception are integrated at two different stages of reach planning, and the sensory weights of each depend on the stage of planning (2003, 2005). First vision and proprioception are combined to create a movement plan based on information about target and hand position. They are again combined when the nervous system is creating the motor plan. They found that the combination of sensory weights was very different at each stage of planning, with visual information having the most impact during movement vector planning, whereas proprioceptive weights were the largest when creating a motor command (Sober and Sabes, 2003, 2005). The goal of these theories is to account for all the transformation and integration processes that occur during reach planning. With no one theory incorporating all behavioural and neurophysiological findings, research will continue to try and create a model to describe the process entirely.

2.5 The Fundamentals of Goal Directed Movements

2.5.1 Knowledge of Body Position and End-Effector Location

In order for people to move their hand between two locations they need to know what their current joint angles are and how they need to change. Between the shoulder and elbow joints there are five degrees of freedom. When the arm is positioned in a particular way, each of the five degrees of freedom have a specific angle (Shadmehr and Wise, 2005). If the central nervous system can compute these joint angles based on the proprioceptive information from the muscles, tendons and joint receptors, then through forward kinematics you would be able to compute the hand location (Jordan and Rumelhart, 1992; Jordan et al., 1994; Wise and Shadmehr, 2004), whereas if you wanted to calculate the joint angles based solely on the hands spatial location, the CNS would use inverse kinematics (Jordan and Rumelhart, 1992; Jordan et al.,1994; Shadmehr and Wise, 2005, 2004). Not only can end-effector location be computed through proprioceptive signals, but visual information can provide valuable knowledge as well.

2.5.2 Computing Target Location

To successfully complete any reaching movement, not only is it important to have knowledge about body position, but the target location as well. The target is usually represented in visual coordinates, but in order to use this information to create a movement, it needs to be transformed into a shoulder-based frame of reference. In order to do this, knowledge about where the target falls on the retina, the eye orientation, and head angle relative to the shoulder all need to be taken into account (Blohm and Crawford, 2007). The CNS takes the target information and calculates a difference vector between the location of the hand and the location of the target. The difference vector determines the magnitude and direction that the hand needs to move in order to reach the target.

2.5.3 Visuomotor Transformations for Reaching

Formulating a movement plan requires visual signals to be transformed into a motor plan, while at the same time taking into account full body geometry. Therefore our brain needs to be aware of the eyes rotational position in the orbit, head orientation relative to the shoulder, and limb configuration (Blohm and Crawford, 2007; Blohm et al., 2009). Failure to account for any rotations in head and eye position will result in movement errors (Blohm et al., 2007).

When performing a reaching movement, both the target and hand position need to be mapped relative to the line of sight (Blohm and Crawford, 2007). The posterior parietal cortex (PPC) is thought to be responsible for coding target location based on where the image falls on the retina (Andersen and Buneo, 2002; Batista et al. 1999). This type or representation is referred to as gaze-centered and is dependent on eye and head orientation (Medendorp et al., 2003). Mendendorp and colleagues (2003,2005) conducted a MRI study focusing on goal directed eye and pointing movements and found that the PPC more greatly responds to a task that involves moving towards a remembered target rather than simply just recognizing it. The PPC seems to play a significant role in movement planning and target memorization, thus it should receive target positional information that is representative of eye and head positions. With the same importance, cells in the primary motor cortex (M1) and the dorsal premotor cortex (PMd) respond to changes in hand orientation (Medendorp et al., 2005; Georgeopolos et al. 1982; Wise and Shadmehr, 2002; Churchland et al. 2006). In addition to M1 and PMd playing a role in hand localization, cells in the ventral premotor cortex (PMv) have been found to encode target position relative to the body (Mushiake et al. 1997; Rizzolatti et al. 2002).

The CNS uses this information from areas PPC, M1, PMv and PMd and maps target and hand positions, while subsequently comparing their spatial locations. Noting that PM and M1 do not represent movement plans in visual coordinates. This information is used to compute a difference vector, that is then used to create a movement plan. According to Sober and Sabes, the movement plan is represented in visual coordinates and must be transformed into a shoulder-centered frame of reference in order for it to be executed (2003, 2005).

2.5.4 Transforming Movement Vector into a Trajectory

Once the movement plan is represented in shoulder-centered coordinates, the motor system needs to determine what dynamic computations need to occur in order to achieve the goal (Wise and Shadmehr, 2002). Although many cortical areas contribute to motor function, the primary motor cortex receives the greatest amount of input from other cortical regions involved in motor planning and its output to the corticospinal tract is the largest (Scott, 2003; Scott 2004; Porter and Lemon, 1993). In addition to neurons in the primary motor cortex (M1) being tuned to postural signals, they also express activity in relation to the magnitude, direction, speed and force of movement (Wise and Shadmehr, 2002; Fu et al. 1995; Scott et al. 2001; Kalaska et al. 1989).

Although M1 is primarily involved in transforming a movement plan into an actual motor behaviour, it does not activate the muscles directly (Scott, 2004; Wise and Shadmehr, 2002). Alternatively, the signals are sent through the spinal cord, ultimately having an influence on the activity of motoneurons. Electrical signals carrying dynamic information about muscle pattern activation pass from the motoneurons through the neuromuscular junction where they are converted into chemical energy that directly affects the muscle fibers (Rose and Christina, 2006; Hall and Sanes,1993).

2.6 Objectives and Predictions

The objective of this research was to determine if extra-retinal signals, such as head roll, influence perception and action. Previous microneurography studies have examined how altering joint angles affect the proprioceptive afferent firing patterns (Cordo et al., 2002; Burke et al. 1978; Edin and Vallbo 1990). The results indicate that increasing joint angles are accompanied by a rise in muscle spindle firing rates (Cordo et al., 2002; Burke et al. 1978; Edin and Vallbo 1990). The experimental data reveals a visible increase in firing rates which are accompanied by increases in noise. These results lend themselves to the hypothesis that as muscles in the neck are stretched due to increasing head roll angle, the amount of noise that is associated with the signal should increase as well. Based on this rational, we wanted to test if signal-dependant noise activated by head roll would affect how individuals perceive themselves within their environment, as well how this noise affects the weighting and integration of sensory information. The following experiments set out to investigate these inquiries and to provide evidence that can justify our speculations.

Chapter 3

Multi-sensory weights depend on contextual noise in reference frame transformations.

3.1 Abstract

During reach planning, individuals integrate multiple senses to generate accurate information about the location of the hand and the target, which is used to generate a movement. Visual and proprioceptive information are combined to determine the location of the hand. The goal of this study was to determine whether multi-sensory integration is affected by extraretinal signals, such as head roll. It is believed that a coordinate matching transformation is required before vision and proprioception can be combined because proprioceptive and visual sensory reference frames do not generally align. This transformation utilizes extraretinal signals about current head roll position, e.g. to convert proprioceptive signals into visual coordinates. Since head roll is an estimated sensory signal with noise, this head roll dependency should introduce additional noise to the transformed signal, reducing its reliability and thus its weight in the multi-sensory integration.

To investigate the role of noisy reference frame transformations on multi-sensory weighting, we developed a novel probabilistic (Bayesian) multi-sensory integration model (based on Sober and Sabes, 2003) that included explicit (noisy) reference frame transformations. We then performed a reaching experiment to test the model's predictions. To test for head-roll dependent multi-sensory integration, we introduced conflicts between viewed and actual hand position and measured reach errors.

Reach variability analysis revealed that eccentric head roll orientations led to an increase of movement variability, consistent with our model. We further found that the weighting of vision and proprioception depended on head roll, which we interpret being a result of signal dependant noise. Consequently, the brain has online knowledge of the statistics of its internal sensory representations. In summary, we show that sensory reliability is used in a context-dependent way to adjust multi-sensory integration weights for reaching.

3.2 Introduction

We are constantly presented with a multitude of sensory information about ourselves and our environment. Using multi-sensory integration, our brains combine all available information from each sensory modality (e.g. vision, audition, somato-sensation, etc.) (Stein and Stanford, 2008; Ernst and Bulthoff, 2004; Ghahramani et al., 1997; Green and Angelaki, 2010). Although this tactic seems redundant, considering that the senses often provide similar information, having more than one sensory modality contributing to the representation of ourselves in the environment reduces the chance of processing error (Ghahramani et al., 1997). It becomes especially important when the incoming sensory representations we receive are conflicting. When this occurs, the reliability assigned to each modality determines how much we can trust the information provided (Ghahramani et al., 1997). Here we explore how context-dependent sensory-motor transformations affect the modality-specific reliability.

Multi-sensory integration is a process that incorporates sensory information to create the best possible representation of ourselves in the environment. Our brain uses knowledge on how reliable each sensory modality is, and weights the incoming information accordingly (Kording and Wolpert, 2006; Stein and Meredith, 1993; Stein and Stanford, 2008). Bayesian integration is an approach that assigns these specific weights in a statistically optimal fashion based on how reliable the cues are (Ernst and Banks, 2002; Knill and Pouget, 2004; Mon-Williams et al., 1997). For example, when trying to figure out where our hand is, we can use both visual and proprioceptive (i.e. sensed) information to determine its location (Sober and Sabes, 2003, 2005; Ren et al., 2006, 2007). When visual information is available it is generally weighted more heavily than proprioceptive information due to the higher spatial accuracy that is associated with it (Hagura et al., 2007).

Previous studies have used reaching tasks to specifically examine how proprioceptive and visual information is weighted and integrated (Sober and Sabes, 2003, 2005; van Beers et al., 1999). When planning a reaching movement, knowledge about target position relative to the starting hand location is required to create a movement vector. This movement vector is then used to calculate how joint angles have to change for the hand move from the starting location to the target position using inverse kinematics and dynamics (Jordan and Rumelhart, 1992; Jordan et al., 1994). The assessment of target position is generally obtained through vision, whereas initial hand position can be calculated using both vision and proprioception (Rossetti et al., 1995). Although it is easy to recognize what different sources of information are used to calculate initial hand position, knowing how this information is weighted and integrated is not.

The problem is that visual and proprioceptive information are encoded differently. It is believed that in order for vision and proprioception to be combined, they must be represented in the same coordinate frame (Buneo and Andersen, 2006). In other words, one set of information will have to be transformed into a representation that matches the other. The question then becomes, what set of information will be encoded into the other? In reaching, it is thought that this transformation depends on the stage of reach planning (Sober and Sabes, 2005). Sober and Sabes proposed a dual-comparison hypothesis describing how information from vision and proprioception could be combined during a reaching task (2003, 2005). They suggest that visual and proprioceptive signals are combined at two different stages. First, when the movement plan is being determined in visual coordinates; and second, when the visual movement plan is transformed into a motor command, i.e. a change in joint angles (proprioceptive coordinates) (Sober and Sabes, 2005). The latter requires knowledge of initial hand position in joint coordinates. They showed that estimating the position of the arm for movement planning relied mostly on visual information, whereas proprioceptive information was more heavily weighted when determining current joint angle configuration to compute the inverse kinematics (Sober and Sabes, 2003). They hypothesized that this difference in sensory weighting between reference frames arises from the cost of transformation between reference frames. This idea is based on the assumption that any transformation induces noise to the transformed signal resulting in lower reliability and therefore lower weighting (Sober and Sabes, 2003).

To test this hypothesis, we performed a reaching experiment similar to the one by Sober and Sabes (2003, 2005). To evaluate the notion that multi-sensory integration occurs, subjects performed a reaching task where visual and proprioceptive information about hand position differed. We expanded Sober and Sabes (2003, 2005) model into a fully Bayesian model to test how reference frame transformation noise affects multi-sensory integration. To behaviourally test this, we introduced context changes by altering the subject's head roll angle. The rationale was that head roll would affect the reference frame transformations that have to occur during reach planning (Blohm and Crawford, 2007) but would not affect the reliability of primary sensory information (i.e. vision or proprioception). This is based on the hypothesis that head orientation signals would be more variable (noisy) for head orientations away from primary (up-right) positions (Van Beuzekom and Van Gisbergen, 2000; Wade and Curthoys 1997; Blohm and Crawford, 2007). This variability could be caused by signal-dependent noise in muscle spindle firing rates, or in vestibular neurons signaling head orientation (Lechner-Steineitner, 1978; Sadeghi et al., 2007; Faisal et al., 2008; Scott and Loeb 1994; Cordo et al, 2002). Importantly, we hypothesized that larger head roll noise would lead to noisier reference frame transformations, which in turn would render any transformed signal less reliable. Our main goal was to determine the effect of head roll on sensory transformations and its consequences for multi-sensory integration weights.

3.3 Materials and Methods

3.3.1 Participants

Experiments were performed on seven participants between 20 and 24 years of age, all of whom had normal or corrected to normal vision. Participants performed the reaching task with their dominant right hand. All of the participants gave their written informed consent to the experimental conditions that were approved by the Queen's University General Board of Ethics.

3.3.2 Apparatus

While seated, participants performed a reaching task in an augmented reality setup (Figure 1A) using a Phantom Haptic Interface 3.0L (Sensable Technologies; Woburn, Massachusetts). Their heads were securely positioned using a mounted bite bar that could be adjusted vertically (up/down), tilted forward and backward (head pitch), and rotated left/right (head roll to either shoulder). Subjects viewed stimuli that were projected onto an overhead screen through a semi-mirrored surface (Figure 1A). Underneath this mirrored surface was an opaque board that prevented the subjects from viewing their hand. In order to track reaching movements, subjects grasped a vertical handle (attached to the Phantom Robot) mounted on an air sled that slid across a horizontal glass surface at elbow height.

Eye movements were recorded using electrooculography (EOG), (16-channel Bagnoli EMG system; DELSYS; Boston, MA). Two pairs of electrodes were placed on the face, (Blue Sensor M; Ambu; Ballerup, Denmark). The first set was located on the outer edges of the left and right eyes to measure horizontal eye movements. The second pair was placed above and below one of the subject’s eyes to measure vertical eye movements. An additional ground electrode was placed on the first lumbar vertebrae, to record external electrical noise (Dermatrode; AMERICAN IMEX; Irvine, CA).

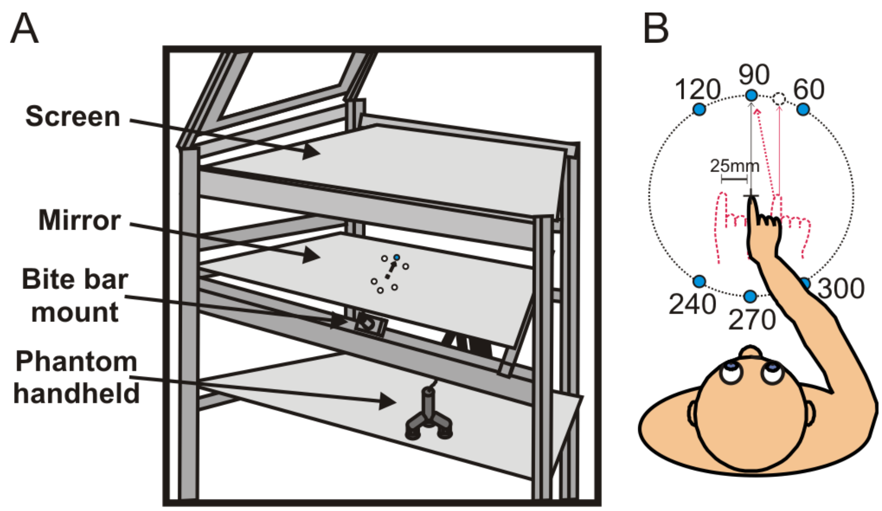

Figure 1: Experimental set up and apparatus.
(A) Experimental apparatus. Targets were displayed on semi-silvered mirror. Subjects head position was kept in place using a bite bar. Reaches were made below the semi-silvered mirror using the Phantom robot. (B) A top view of the subject with all possible target positions. Initial hand positions are shown (-25, 0 and 25mm). Subjects began each trial by aligning their finger with the center cross, and then continued by reaching to one of six targets that would appear. (See text for details)

3.3.3 Task Design

Subjects began each trial by aligning a blue dot (0.5cm) on the display that represented their unseen hand position with a start position cross that was positioned in the center of the display field. The hand circle was only visible when hand position was within 3cm of the central cross. Once the hand was in this position, one of six peripheral targets (1.0cm white dots) would randomly appear 0-250ms later. The appearance of a target was accompanied with an audio cue. At the same time the center cross turned yellow. Once the subject's hand began to move the hand cursor disappeared. Subjects were instructed to perform rapid reaching movements toward the visual targets while keeping gaze fixated on the center position (cross). Targets were positioned at 10 cm distance from the start position cross at 60, 90, 120, 240, 270 and 300 degrees (see Figure 1B).

Once the subject's reach crossed the 10 cm target circle, an audio cue would indicate that they successfully completed the reach, and the center cross would disappear. If subjects were too slow at reaching this distance threshold (more than 750ms after target onset), a different audio cue was played, indicating that the trial was aborted and would have to be repeated. At the end of each reach subjects had to wait 500ms to return to the start position, an audio cue indicated the end of the trial, and the center cross reappeared. This was to ensure subjects received no visual feedback of their performance. Subjects were instructed to fixate the central start position cross (initial hand position cross) throughout the trial.

Subjects completed the task at three different head roll positions, -30 (left), 0 and 30 (right) degrees head roll toward the shoulders (mathematical angle convention from behind subject view). Throughout each head roll condition the proprioceptive information about hand position was altered at random trials, 2.5cm left or right of the visual hand marker. Subjects were not aware of the initial hand position shift when asked after the experiment. We introduced this discrepancy between visual and actual hand position to gain insight into the relative weighting of both signals in the multi-sensory integration process. A similar experiment has been done by Sober and Sabes (2003, 2005). For each hand offset subjects reached to each target twenty times, and they did this for each head roll. Subjects completed 360 trials at each head position, for a total of 1080 reaches. Head roll was constant within a block of trials.

3.3.4 Data Analysis

Eye and hand movements were monitored online at a sampling rate of 1000Hz (16-channel Bagnoli EMG system, DELSYS; Boston, MA; Phantom Haptic Interface 3.0L; Sensable Technologies; Woburn, Massachusetts). Offline analyses were performed in MATLAB (The Mathworks, Natick, MA). Arm position data was low-pass filtered (autoregressive forward–backward filter, cutoff frequency = 50 Hz) and differentiated twice (central difference algorithm) to obtain hand velocity and acceleration. Each trial was visually inspected to ensure that eye movements did not occur while the target was presented (Figure 2C). If they did occur, the trial would be removed from the analysis. Approximately 5% percent of trials (384 of 7560 trials) were removed due to eye movements. Hand movement onset and offset were identified based on a hand acceleration criterion (500mm/s^2), and could be adjusted after visual inspection (Figure 2E). The movement angle was calculated through regression of the data points from the initial hand movement until the hand crossed the 10 cm circle

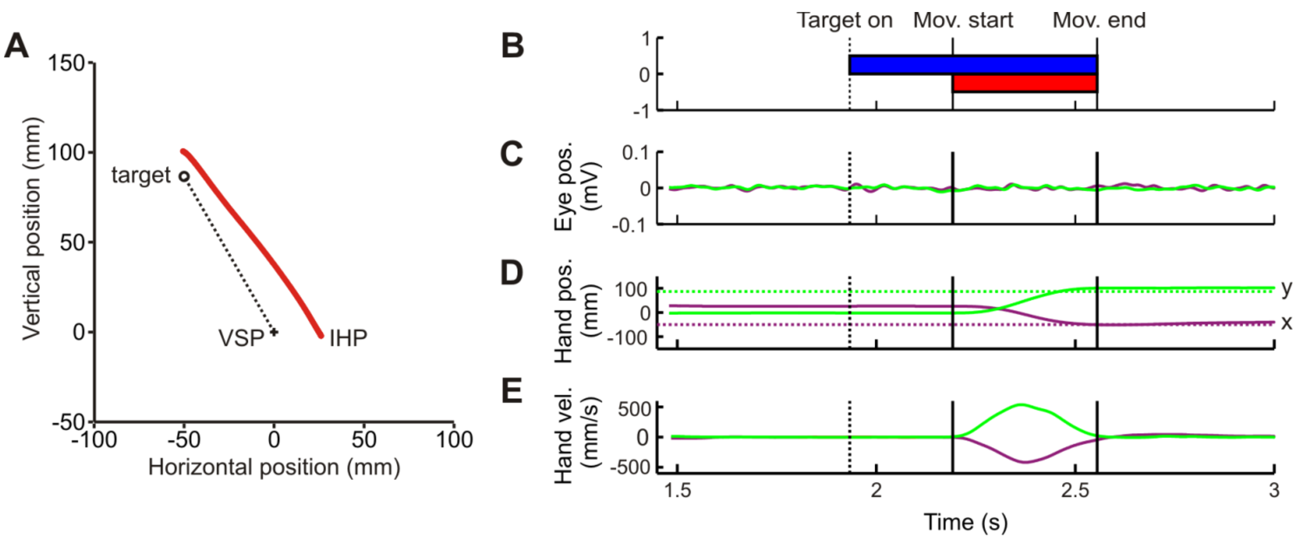

Figure 2: Typical subject trial
(A) Raw reach data from a typical trial displayed. The viewed required reach (dotted line) begins at the cross (visual start position, VSP), and ends at the target (open circle). The red line represents the subjects actual hand position. The subject starts this reach with an initial hand position (IHP) offset to the right by 25mm. **(B)** Target onset and display. Timing of the trial begins when the subject aligns the hand cursor with the visual start position. The target then appears, and remains on until the end of the trial. Movement onset, as well as offset times are shown by the vertical lines. **(C)** Eye movement traces. Horizontal (purple) and vertical (green) eye movement traces, from EOG recordings. Subjects were instructed to keep the eyes fixated on the VSP for the entire length of the trial. Black vertical lines indicate arm movement start and end. **(D)** Hand position traces. Horizontal (purple) and vertical (green) hand positions (solid lines) as well as the horizontal and vertical target position (dotted lines) are plotted over time. **(E)** Hand velocity traces relative to time.

around the initial hand position cross. Directional movement error was calculated as the difference between overall movement angle and visual target angle.

3.3.5 Modelling the Overall Movement Direction

The data was fitted to two models, one previously published velocity command model (Sober and Sabes, 2003) and a second fully Bayesian model that had similar processing steps than Sober and Sabes (2003) but in addition included explicit reference frame transformations and – more importantly – explicit transformations of the sensory noise throughout the model. Below, we outline the general working principle of the model; please refer to Appendix 1 for model details.

The purpose of these models was to determine the relative weighting of both vision and proprioception during reach planning, separately for each head roll angle. Sober and Sabes (2003, 2005) proposed that initial hand position is computed twice, once in visual and once in proprioceptive coordinates (Figure 3A). In order to determine the initial hand position in visual coordinates (motor planning stage, left dotted box in Figure 3A), proprioceptive information about the hand must be transformed into visual coordinates (Figure 3A, red "T" box) using head orientation information. Both visual and the transformed proprioceptive information are weighted based on reliability, and initial hand position is calculated. This initial hand position can then be subtracted from the target position to create a desired movement vector (Δx). If the hand position is misestimated (due to initial hand position offset), then there will be an error associated with the desired movement vector.

In a final processing step, this movement vector will undergo a transformation to be represented in a shoulder based reference frame (Figure 3A, $T_{V \rightarrow P}$ box). Initial joint angles are calculated by transforming visual information about hand location into proprioceptive coordinates (Figure 3A, rightward arrows through red “T” box). This information is weighted along with the proprioceptive information, to calculate initial hand position in proprioceptive coordinates (right dotted box in Figure 3A) and is used to create an estimate of initial elbow and shoulder joint angles (θ initial). Using inverse kinematics, a change in joint angles ($\Delta\theta$), from the initial starting position to the target is calculated based on the desired movement vector. Since the estimate of initial joint angles (θ initial) is needed to compute the inverse kinematics, misestimation of initial joint angles will lead to errors associated with the inverse kinematics, and therefore error in the movement. We wanted to see how changing head roll would affect the weighting of visual and proprioceptive information. As can be seen from Figure 3A, our model reflects the idea that head orientation affects this transformation. This is because we hypothesize (and hope to demonstrate this through our data) that transformations add noise to the transformed signal and that the amount of this noise depends on the amplitude of the head roll angle. Therefore, we predict that head roll has a significant effect on the estimations of initial hand position, thus changing the multi-sensory integration weights and in turn affecting the accuracy of the movement plan.

3.4 Results

To test the model’s predictions, we asked participants to perform reaching movements while we varied head roll and dissociated visual and proprioceptive initial hand positions.

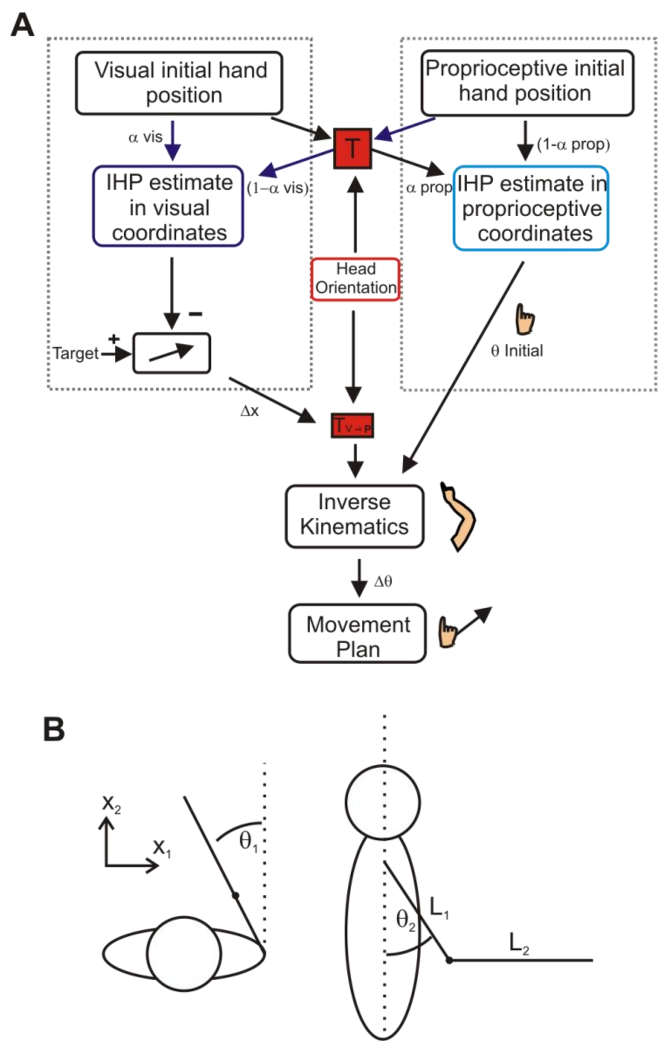

Figure 3: Multi-sensory integration model.
(A) Model for multi-sensory integration for reach planning. In order to successfully complete a reach, hand position estimates have to be calculated in both proprioceptive (right dotted box) and visual coordinates (left dotted box). Initial hand position estimates in visual coordinates are computed by transforming proprioceptive information into visual coordinates (transformation "T"). Visual and proprioceptive information is then weighted and combined (visual weights α; proprioceptive weights α-1). The same processes happen for proprioceptive IHP estimates; only this time visual information is transformed into proprioceptive coordinates. Subtracting visual IHP from the visual target location, a movement vector can be created. Using inverse kinematics, the movement vector is combined with the calculation of initial joint angles, derived from the IHP in proprioceptive coordinates to create a movement plan based on changes in joint angles. **(B)** Spatial arm position (x) can be characterized in terms of two joint angles**,** deviation from straight ahead (θ_1) and upper arm elevation (θ_2). The arm and forearm lengths are represented by "L". (See text for details)

3.4.1 General Observations

A total of 7560 trials were collected, with 384 trials being excluded due to eye movements. Subjects were unaware of the shifts in initial hand position. We used reaching errors to determine how subjects weighted visual and proprioceptive information. Reach error (in angular degrees) was computed as angle between the movement and the visual hand-target vector, where 0deg error would mean no deviation from the visual hand-target direction. As a result of the shifts in the actual starting hand locations, a situation was created where the subject received conflicting visual and proprioceptive information. Based on how the subject responded to this discrepancy, we could determine how information was weighted and integrated.

Figure 4 displays nine sets of raw data reaches from a typical subject, depicting 10 reaches to each target. Every tenth data point is plotted for each reach, i.e. data points are distant in time by 10ms, allowing the changes in speed to be visually identifiable. The targets are symbolized by black circles, with the visual start position marked by a cross. Each set of reaches is representative of a particular head roll angle (rows) and initial hand position (columns). One can already observe from these raw traces that this subject weighted visual initial hand position more than proprioceptive information resulting in a movement path that is approximately parallel to a virtual line between the visual cross and target locations.

To further analyze this behavior, we compared the reach error (in degrees) for each hand offset condition (Figure 5A). This graph also displays a breakdown of the data for each target angle and shows a shift in reach errors between the different initial hand positions. The difference in reach errors between the each of the hand offsets indicates

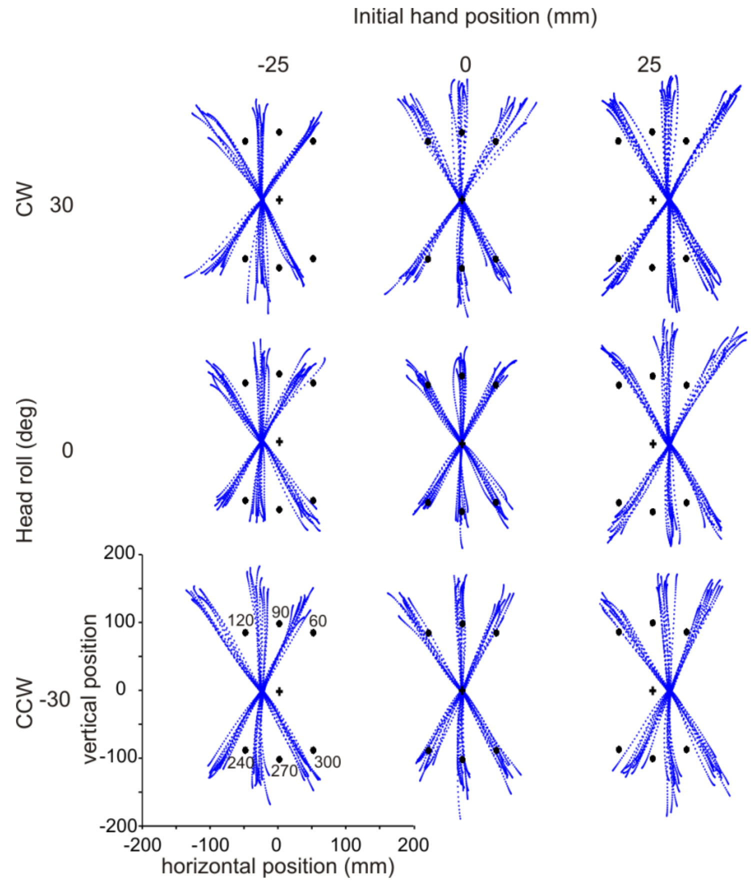

Figure 4: Raw reaches from a typical subject.
Each grouping of reaches corresponds to a particular head orientation (30°, 0°, -30°) and initial hand position (-25mm, 0mm, 25mm). In each block, ten trials are plotted for each target (black dots). Target angles are 60°, 90°, 120°, 240°, 270°, and 300°. The data points for each reach trajectory represent every tenth data point.

that both visiual and proprioceptive information were used during reach planning. Figure 5B shows a fit from Sober and Sabes' (2003, 2005) previously proposed model to the normalized data from figure 5A (see also Appendix 1 for model details). The data from figure 5A were normalized to zero by subtracting the zero hand offset from the initial hand positions 25mm and -25mm. Sober and Sabes' (2003) previously proposed velocity command model fit our data well. In figure 5B, it is clear that the normalized data points for each hand position follow the same pattern as the model predicted error, represented by the dotted lines. Based on this close fit of our data to the model, we can now use use this model in a first step to investigate how head roll affects the weighting of vision and proprioceptive information about the hand.

3.4.2 Head Roll Influences on Reach Errors

As mentioned before, subjects performed the experiment described above for each head roll condition, i.e. -30, 0 and 30 degrees head roll (to the left shoulder, upright and to the right shoulder respectively). We assumed that if head roll was not taken into account, there would be no difference in the reach errors between the head roll conditions. However, Figure 6 does not display this trend. There are differences in reach errors between the different head roll conditions, indicating that head roll was a factor influencing reach performance. However, this is a novel finding that has never been considered in any previous model.

From our model (Figure 3A), we predicted that as head roll moves away from zero, more noise would be associated with the signal (Blohm and Crawford 2007; Scott and Loeb, 1994; Tarnutzer et al. 2009). This increase in noise should affect the overall movement variability (i.e. standard deviation, SD) because more noise in the head roll

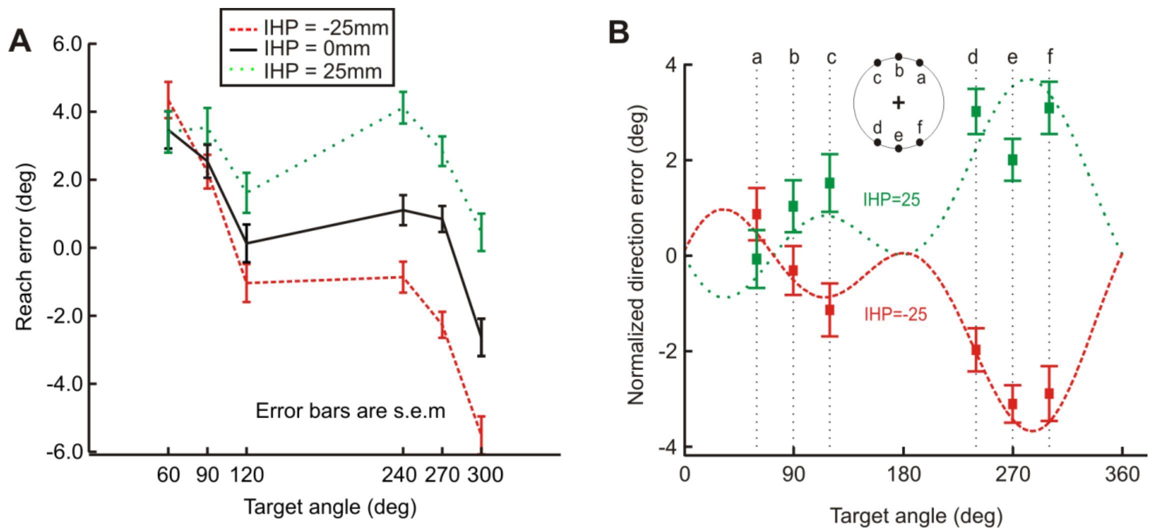

Figure 5: Hand offset effects
(A) This graph demonstrates a shift in reach errors between each initial hand position (-25mm, 0mm, 25mm), suggesting that visual and proprioceptive information are both used when reaching. **(B)** Model fit. The data from A was normalized to zero, and plotted against the model fit (dotted lines; initial hand position 25 (green) and -25 (red)). The squared points represent the normalized direction error for each initial hand position at each target angle. This graph demonstrates that the model previously proposed by Sober and Sabes (2003) fits our data. Error bars represent standard error of the mean.

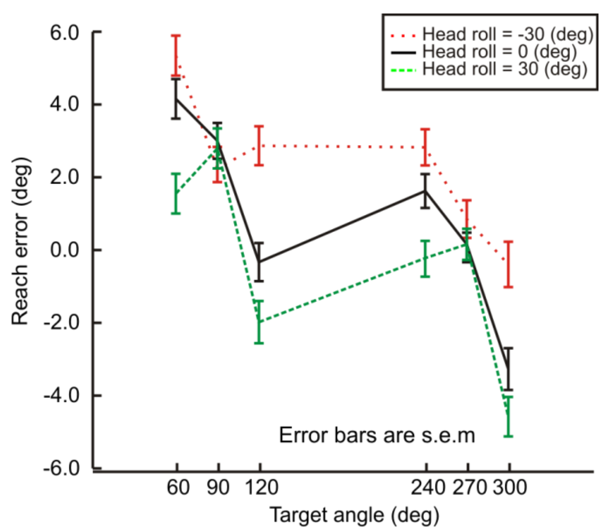

Figure 6: Head roll effects
Reach errors are plotted for each head roll (-30°, 0°, 30°) at each target angle (60°,90°,120°,240°,270°,300°). The difference in reach error indicates that information about head roll in taken into account. Error bars represent standard error of the mean.

signal should result in more noise added during the reference frame transformation process. Figure 7 plots movement variability for trials where the head was upright compared to rolled to the left or right combined. We performed a paired t-test between head roll and no head roll conditions across all 7 subjects and all hand positions (21 standard deviation values per head roll conditions). Across all three initial hand positions, movement variability was significantly greater when the head was rolled compared to when the head was straight $t(20)=-3.512$, $p<0.01$. This was a first indicator that head roll introduced signal-dependent noise to motor planning, likely through noisier reference frame transformations (Blohm and Crawford, 2007; Sober and Sabes, 2003, 2005).

If changing the head roll angle ultimately affects reach variability, then we would expect that the information associated with the increased noise would be weighted less at the multi-sensory integration step. To test this, we fitted Sober and Sabes' (2003) model on our data independently for each head orientation. The visual weights, of initial hand positions represented in visual (dark blue, α_{vis}) and proprioceptive (light blue, α_{prop}) coordinates are displayed in Figure 8A. The visual weights of initial hand position (IHP) in visual and proprioceptive coordinates were significantly different when the head was rolled compared to the head straight condition ($t(20)=-4.217$, $p<0.01$). Visual information was weighted more heavily when initial hand position was calculated in visual coordinates compared to proprioceptive coordinates. Furthermore, visual information was weighted significantly more for IHP in visual coordinates for head rolled conditions, compared to head straight. In contrast, visual information was weighted significantly less when the IHP was calculated in proprioceptive coordinates for head

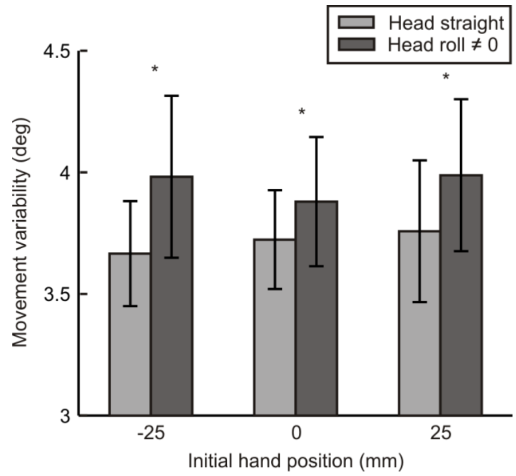

Figure 7: Movement variability as a function of head roll.
For each initial hand position (-25mm, 0mm, 25mm) movement variability (standard deviation) is compared between head straight and head roll conditions (0, ≠0). Reaches when the head is rolled had significantly more variability compared to reaches when the head is straight.

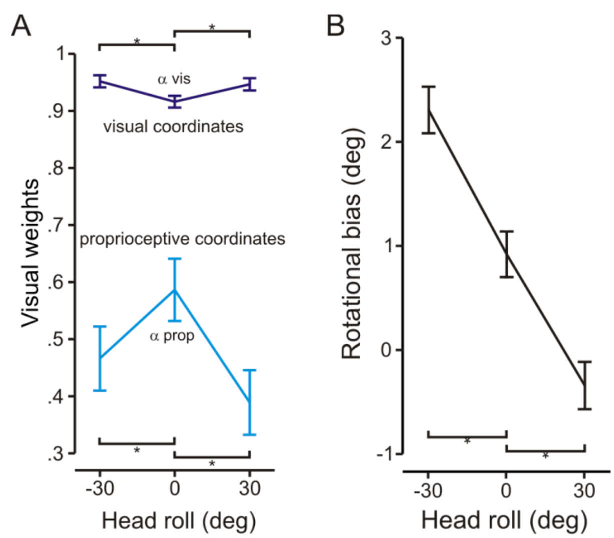

Figure 8: Model fit and rotational biases
(A) The model was fit to the data for each head roll condition. The visual weights for initial hand position estimates are plotted for both visual (dark blue) and proprioceptive (light blue) coordinate frames. Significant differences are denoted by the *(p<0.05). **(B)** Rotational biases are plotted and compared for each head roll position (-30°, 0°, 30°).
added by this transformation, e.g. vision is weighted less in proprioceptive as opposed to visual coordinates (Sober and Sabes, 2003, 2005). An even further reduction of weighting of the transformed signal will occur if head roll is introduced, presumably due to signal dependant noise (see Discussion section).

rolled conditions compared to head straight. This finding is representative of the fact that information that undergoes a noisy transformation is weighted less due to the noise.

In addition to accounting for head roll noise, the reference frame transformation also have to estimate the amplitude of the head roll angle. Any misestimation in head roll angle will lead to a rotational movement error. Figure 8B plots the rotation biases (i.e. the overall rotation in movement direction relative to the visual hand-target vector) for each head roll position. The graph shows that there is a rotational bias for reaching movements even for 0deg head roll angle. This bias changes depending on head roll. There were significant differences between the rotational biases for head roll conditions compared to head straight ($t(20)>6.891$, $p<0.01$).

3.4.3 Modeling Noisy Reference Frame Transformations

We developed a full Bayesian model of multi-sensory integration for reach planning. This model uses proprioceptive and visual initial hand position (IHP) estimates and combines them in a statistically optimal way, separately in two different representations (Sober and Sabes, 2003; 2005): proprioceptive coordinates and visual coordinates (Figure 3B). After combination, IHP in visual coordinates is compared to target position in visual coordinates to generate a desired movement vector. Using current joint configuration from the multi-sensory integration in proprioceptive coordinates, we then compute the movement using a velocity command model (Sober and Sabes, 2003; 2005).

Compared to previous models (Sober and Sabes, 2003; 2005), our model includes two crucial additional features. First, we explicitly include the required reference transformations (Figure 3A, “T”) from proprioceptive to visual coordinates (and vice versa), including the forward/inverse kinematics for transformation between Euclidean space and joint angles as well as for movement generation. The reference frame transformation T depends on an estimate of body geometry, i.e. head roll angle (Figure 3A, “H”) in our experiment. Second, in addition to modeling the mean behavior, we also include a full description of variability. Visual and proprioceptive sensory information have associated noise, i.e. proprioceptive and visual IHP as well as head roll angle. As a consequence, covariance matrices of all variables also have to undergo the above-mentioned transformations. In addition, these transformations themselves are noisy, i.e. they depend on noisy sensory estimates.

To illustrate how changes in transformation noise, visual noise and joint angle variability affect predicted reach error, we used the model to simulate these conditions. We did this first to demonstrate that our model can reproduce the general movement error pattern produced by previous models (Sober and Sabes, 2003) and second to show how different noise amplitudes in the sensory variables change this error pattern. Figure 9A displays the differences in predicted error between high, medium and low noise in the reference frame transformation. As the amount of transformation noise increases, the reach error decreases. The transformed signal in both visual and proprioceptive coordinates is weighted less in the presence of higher transformation noise. However, the misestimation of initial hand position in visual coordinates has a bigger impact on movement error than the IHP estimation in proprioceptive coordinates (Sober and Sabes, 2003, 2005). As a consequence, the gross effect of higher transformation noise is a decrease in movement error because the proprioceptive information will be weighted relatively less after it is converted into visual coordinates.

Figure 9B illustrates the effect of visual sensory noise (e.g. in situations such as seen versus remembered stimuli) on predicted error in a high transformation noise condition. When the amount of visual noise increases (visual reliability decreases), proprioceptive information will be weighted more, and predicted error will increase. Conversely, as visual noise decreases (reliability increases), predicted error will decrease as well. Differences seen between different movement directions (forward and backward) are due to an interaction effect of transformations for vector planning (visual coordinates) and movement execution (proprioceptive coordinates).

Not only does visual noise impact the predicted error, but proprioceptive information does as well. Noise associated with different joint angles will result in proprioceptive information being weighted less than visual information, and as a result there will be a decrease in predictive error (Figure 9C). Figure 9C displays how changing the amount of noise associated with one joint angle over another can change the predicted error. For example with $\theta_1 > \theta_2$, the signals indicating the arm deviations from the straight ahead position are noisier than the signals indicating upper arm elevation. With this situation, visual error will be smaller when the targets are straight ahead or behind because the proprioceptive signals for the straight ahead position are noisier and thus will be weighted less.

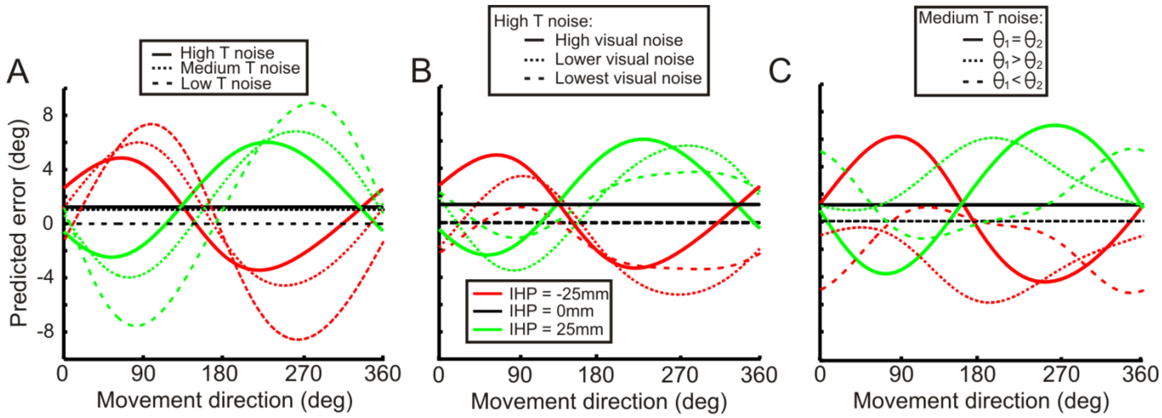

Figure 9: Model simulations

Each graph illustrates how different stimulus parameters affect the predicted reach error for each of the initial hand positions (-25, 0, 25). **(A)** Low, medium and high transformation noise is compared. **(B)** Different magnitudes of visual noise affect predicted error in the high transformation noise condition. **(C)** Different amounts of noise associated with separate joint angles affects predicted error in the medium transformation noise condition.

Figure 10 displays the model fits to the data for both error (top panels) and variability (lower panels) graphs for each initial hand position (-25mm, 0mm, 25mm), comparing the different head roll effects. The solid lines represent the model fit for each initial hand position, with the squared nodes representing the behavioral data for each target. The model fits are different for each head roll position, with zero head roll falling in between the tilted head positions. The model predicts that -30deg head roll and 30deg head roll would have reach errors in opposite directions; this is consistent with the data. Furthermore, the model presents zero head roll as having the least variability when reaching towards the visual targets, with the behavioral data following the same trend.

In addition to modeling the effect of head roll on error and variability, we plotted the differences for initial hand positions (IHP) as well. Figure 11 displays both error and variability graphs for each head roll condition (same plots as in Figure 10, but re-arranged according to head roll conditions). The reach errors for different IHPs changed in a systematic way; however differences in variability between the initial hand positions are small and show a similar pattern of variability across movement directions.

Determining how head roll affects multi-sensory weights was the main goal of this experiment. Previously in this section we fitted Sober and Sabes' (2003) original model to the data, and displayed the visual weights for initial hand position estimates for both visual and proprioceptive coordinate frames (Figure 8A). In our model, we did not explicitly fit those weights to the data; however, from the covariance matrices of the sensory signals, we could easily recover the multi-sensory weights (see Appendix 1). Since our model uses 2-dimensional covariance matrices (a two dimensional environment allows a visual coordinate frame to be represented in x and y, and

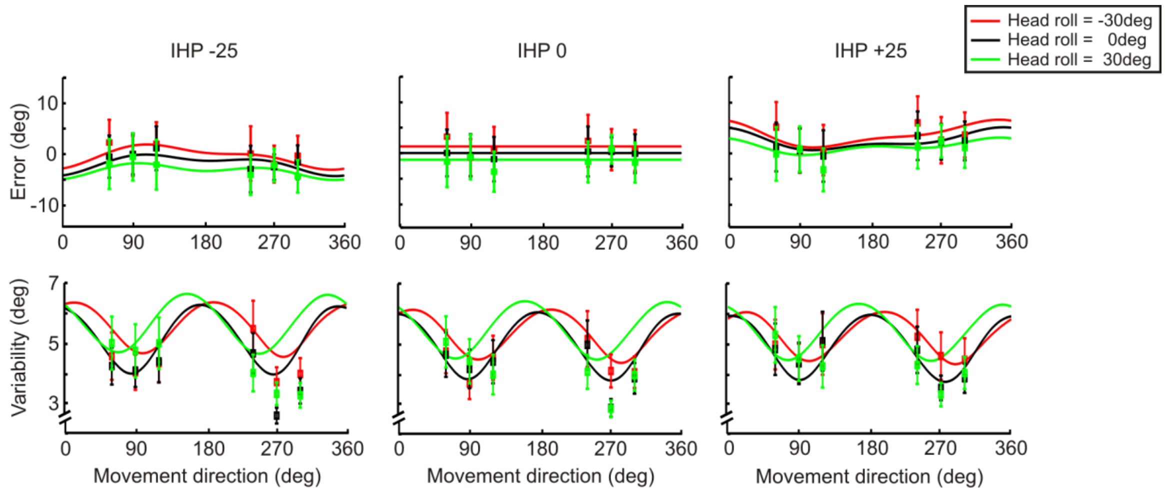

Figure 10: Model fit comparing head roll conditions
For each initial hand position (-25mm, 0mm, 25mm) both reaching error and variability are plotted. The solid lines represent the model fit for each head roll; -30° (red), 0° (black) and 30° (green). The squared points represent the data sampled at each target angle (60°, 90°, 120°, 240°, 270°, 300°).

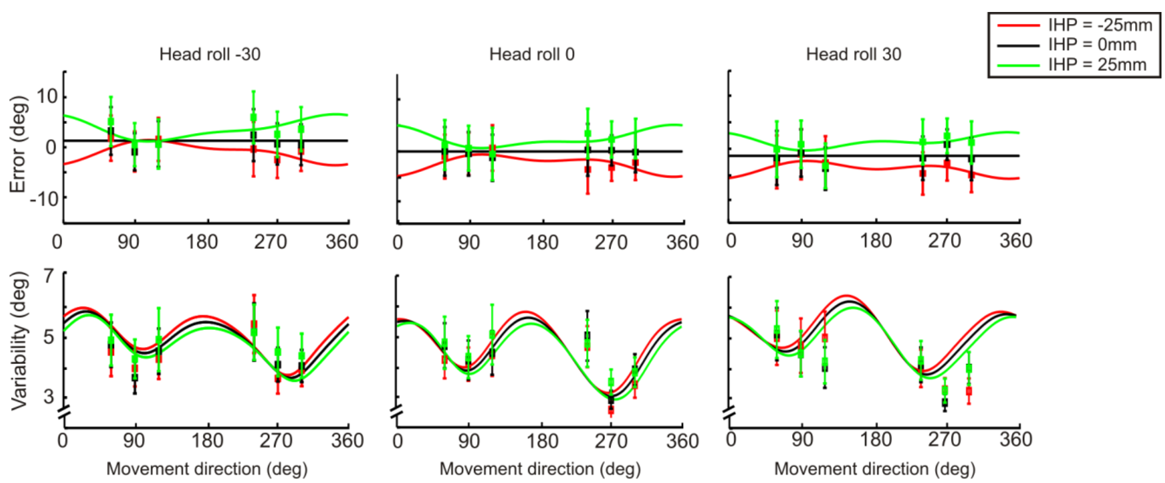

Figure 11: Model fit comparing different initial hand positions
For each head roll angle (-30°, 0°, 30°) both reaching error and variability are plotted. The solid lines represent the model fit for each initial hand position; -25mm (red), 0mm (black) and 25mm (green). The squared points represent the data sampled at each target angle (60°, 90°, 120°, 240°, 270°, 300°). Data re-arranged from figure 10.

proprioceptive coordinates to be displayed by two joint angles), the recovered multi-sensory weights were also 2D matrices. We used the diagonal elements of those weight matrices as visual weights in visual (x and y) and proprioceptive (joint angles) coordinates. Figure 12 displays significant differences ($t(299)<-10$, $p<0.001$) for all visual weights between head straight and head rolled conditions, except for Θ_2. Visual weights were higher for visual coordinates when the head is rolled. In contrast, visual weights decrease in proprioceptive coordinates when the head is rolled compared to the head straight condition. These results were very similar to the original model fits performed in Figure 8A. Thus, our model was able to simulate head-roll dependent noise in reference frame transformations underlying reach planning and multi-sensory integration. More importantly, our data show that head-roll dependent noise can influence multi-sensory integration in a way that is explained through context-dependent changes in added reference frame transformation noise.

3.4.4 Discussion

In this study, we analyzed the effect of context-dependent head roll on multi-sensory integration during a reaching task. We found that head roll influenced reach error and variability in a way that could be explained by signal-dependent noise in the coordinate matching transformation between visual and proprioceptive coordinates. To demonstrate this quantitatively, we have developed the first integrated model of multi-sensory integration and reference frame transformations in a probabilistic framework. This shows that the brain has online knowledge of the uncertainty associated with each sensory variable and uses this information to plan motor actions in a statistically optimal fashion (in the Bayesian sense).

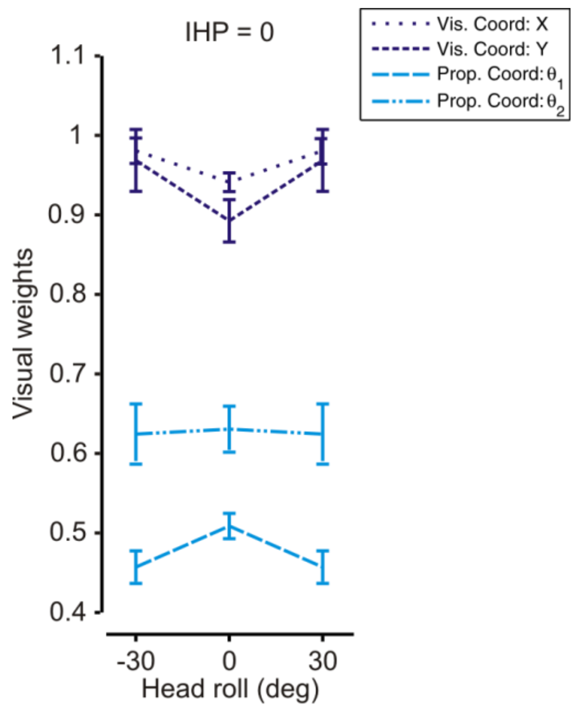

Figure 12: 2D model fit for each head roll
The model was fit to the data for each head roll condition. The visual weights for initial hand position estimates are plotted for visual (dark blue) and proprioceptive (light blue) coordinate frames with standard deviations. A two dimensional environment allows visual x and y and proprioceptive θ_1 and θ_2 to be weighted separately. There were significant differences in visual weighting between head straight and head roll conditions for all coordinate representations except proprioceptive θ_2.

3.4.5 Experimental Findings

When we changed the hand offset, we found reach errors that were similar to previously published data in multi-sensory integration tasks (Sober and Sabes, 2003, 2005; McGuire and Sabes, 2009) and were well described by Sober and Sabes' (2003) model. In addition we also found changes in the pattern of reach errors across different head orientations. This was a new finding that previous models did not explore. There were multiple effects of head roll on reach errors. First, there was a slight rotational offset for the head straight condition, which could be a result of biomechanical biases, e.g. related to the posture of the arm. In addition, our model-based analysis showed that reach errors shifted with head roll. Our model accounted for this shift by assuming that head roll was over-estimated in the reference frame transformation during the motor planning process. The over-estimation of head roll could be explained by ocular counter-roll. Indeed, when the head is held in a stationary head roll position, ocular counter-roll compensates for a portion of the total head rotation (Bockisch and Haslwanter, 2001; Collewijn et al., 1985; Haslwanter et al., 1992). This means that the reference frame transformation has to rotate the retinal image less than the head roll angle. Not taking ocular counter-roll into account (or only partially accounting for it) would thus result in an over-rotation of retinal image, similar to what we observed in our data. However, since we did not measure ocular torsion, we cannot evaluate this hypothesis.

The second effect of head roll was a change in movement variability. Non-zero head roll angles produced reaches with higher variability compared to reaches during upright head position. This occurred despite the fact that the quality of the sensory input from the eyes and arm did not change. We took this as evidence for head roll influencing the sensory-motor reference frame transformation. Since we assume head roll to have signal-dependent noise (see below), different head roll angles will result in different amounts of noise in the transformation.

Third and most importantly, head roll changed the multi-sensory weights both at the visual and proprioceptive processing stages. This finding was validated independently by fitting Sober and Sabes' (2003) original model and our new full Bayesian reference frame transformation model to the data. This is evidence that head roll variability changes for different head roll angles and that this signal-dependent noise enters the reference frame transformation and adds to the transformed signal, thus making it less reliable. Therefore, the context of body geometry influences multi-sensory integration through stochastic processes in the involved reference frame transformations.

Signal-dependent head roll noise could arise from multiple sources. Indeed, head orientation can be derived from vestibular signals as well as muscle spindles in the neck. The vestibular system is an essential component for determining head position sense; specifically the otolith organs (utricle and saccule) respond to static head positions in relation to gravitational axes (Fernandez et al., 1972; Sadeghi et al., 2007). We suggest that the noise from the otoliths varies for different head roll orientations; such signal-dependent noise has previously been found in the eye movement system for extra-retinal eye position signals (Li and Matin, 1992; Gellman and Fletcher, 1992). In addition, muscle spindles are found to be the most important component in determining joint position sense (Goodwin et al., 1972, Scott and Loeb, 1994), with additional input from cutaneous and joint receptors (Clarke and Burgess, 1975; Gandevia and

McCloskey, 1976; Armstrong et al. 2008). Muscles found in the cervical section of the spine contain high densities of muscle spindles, enabling a relatively accurate representation of head position (Armstrong et al. 2008). In essence, as the head moves away from an upright position, more noise should be associated with the signal due to an increase in muscle spindle firing (Cordo et al., 2002; Burke et al. 1978; Edin and Vallbo 1990; Scott and Loeb 1994). However, due to the complex neck muscle arrangement, a detailed biomechanical model of the neck (Lee and Terzopoulos, 2006) would be needed to corroborate this claim.

3.4.6 Model discussion

We have shown that noise affects the way reference frame transformations are performed in that transformed signals have increased variability. A similar observation has previously been made for eye movements (Li and Matin, 1992; Gellman and Fletcher, 1992) and visually-guided reaching (Blohm and Crawford, 2007). This validates a previous suggestion that any transformation of signals in the brain has a cost of added noise (Sober and Sabes, 2003, 2005). Therefore, the optimal way for the brain to process information would be to minimize the number of serial computational (or transformational) stages. The latter point might be the reason why multi-sensory comparisons could occur fewer times but in parallel at different stages in the processing hierarchy and in different coordinate systems.

In our model, multi-sensory integration occurred in specific reference frames, i.e. in visual and proprioceptive coordinates. Underlying this multiple comparison hypothesis is the belief that signals can only be combined if they are represented in the same reference frame (Buneo and Andersen, 2006; Cohen and Andersen, 2002; Engel et al., 2002; Lacquaniti and Caminiti, 1998; McGuire and Sabes, 2009). However, this claim has never been explicitly verified and this may not be the way neurons in the brain actually carry out multi-sensory integration. The brain could directly combine different signals across reference frames in largely parallel neural ensembles (Blohm et al., 2009; Deneve, Latham and Pouget, 2001), for example using gain modulation mechanisms (Andersen and Mountcastle, 1983; Chang et al., 2009). Regardless of the way the brain integrates information, the behavioral output would likely look very similar. A combination of computational and electro-physiological studies would be required to distinguish these alternatives.

Our model is far from being complete. In transforming the statistical properties of the sensory signals through the different processing steps of movement planning, we only computed first-order approximations and hypothesized that all distributions remained Gaussian. This is of course a gross over-simplification; however, no statistical framework for arbitrary transformations of probability density functions exists. In addition, we only included relevant 2D motor planning computations. In the real world, this model would need to be expanded into 3D with all the added complexity (Blohm and Crawford, 2007), i.e. non-commutative rotations, offset between rotation axes, non-linear sensory mappings and 3D behavioral constraints (such as Listing’s law).

3.4.7 Implications

Our findings have implications for behavioral, perceptual, electrophysiological and brain imaging experiments. First, we have shown behaviorally, that body geometry signals can change the multi-sensory weightings in reach planning. Therefore, we also expect other contextual variables to have potential influences, such as gaze orientation, task/object value or attention (Sober and Sabes, 2005). Second, we have shown contextual influences on multi-sensory integration for action planning, but the question remains whether this is a generalized principle in the brain that would also influence perception.

Finally, our findings have implications for electrophysiological and brain imaging studies. Indeed, when identifying the function of brain areas, gain-like modulations in brain activity are often taken as an indicator for reference frame transformations. However, as previously noted (Deneve et al., 2001), such modulations could also theoretically perform all kinds of other different functions involving the processing of different signals, such as attention, target selection or multi-sensory integration. Since all sensory and extra-sensory signals involved in these processes can be characterized by statistical distributions, computations involving these variables will evidently look like probabilistic population codes (Ma et al., 2006) – the suggested computational neuronal substrate of multi-sensory integration. Therefore, the only way to determine if a brain area is involved in multi-sensory integration is to generate sensory conflict and analyze the brain activity resulting from this situation in conjunction with behavioral performance (Nadler et al., 2008).

3.4.8 Conclusions

In examining the effects of head roll on multi-sensory integration, we found that the brain incorporates contextual information about head position during a reaching task. We developed a new statistical model of reach planning combining reference frame transformations and multi-sensory integration to show that noisy reference frame transformations can alter the sensory reliability. This is evidence that the brain has online knowledge about the reliability of sensory and extra-sensory signals and includes this information into signal weighting, to ensure statistically optimal behavior.

Chapter 4

Head roll influences perceived location of hand position

4.1 Abstract

Theoretical and electrophysiological studies of motor planning have suggested that the brain can only compare or integrate different sensory signals if they are represented in a common frame of reference; however, this idea has never been explicitly tested for perception. Perceiving felt (proprioceptive) hand location relative to some (e.g. visual) landmark would thus require both signals to be first converted into a common reference frame. We have previously shown (Burns and Blohm, SfN2009) that such reference frame conversions can induce body-geometry-dependent noise. This noise in turn alters the sensory reliability during action planning. Here, we examine whether extraretinal signals, specifically head roll, also alter sensory perception through a similar mechanism. To do so, we examine the accuracy of visual localization relative to proprioceptive hand position for different head roll orientations.

Seven healthy (right handed) subjects were required to judge whether their unseen hand was located closer or further and left or right (4-alternative forced choice task) from a visual target. This was done for three different head roll rotations (-30, 0 and 30 deg) by placing both arms within a robotic exoskeleton and measuring flexion and extension of both elbow and shoulder within the horizontal plane. After aligning their hand with a start target, visual hand feedback was removed and the (right) arm was passively moved to a random position located in front of the initial hand position target. Then, a visual target (VT) was briefly presented (500ms) at a random location around

the fingertip and subjects were required to use their left hand to indicate via a virtual response display in which quadrant VT appeared relative to the right hand location.

We show that eccentric head roll increases the uncertainty in the subjects' ability to discriminate target location relative to the fingertip. In addition, subjects showed perceptual biases between the head roll conditions, suggesting that the perception of target locations relative to the finger tip position shifts when the head is rolled to either shoulder. We conclude that sensory perception is sensitive to body-geometry-dependent noise affecting the coordinate matching transformations of the sensory data and thus decreasing the discrimination threshold.

4.2 Introduction

How we perceive our environment crucially affects the way we interact with it. Being able to determine our spatial location relative to the external environment is a necessity for spatial perception and action planning. Vision provides the strongest sensory input to build an internal representation of the outside world, which can be used in both action and perception (Goodale, 1983 as cited in Goodale, In Press). In addition, proprioception creates an awareness of our position sense and allows us to move within our environment even in the absence of vision (Goodwin et al., 1972; Fuentes and Bastian, 2010). For vision and proprioception to be merged into a unique internal representation of ourselves within the environment, it is believed that all sensory signals have to be converted into a common frame of reference (Blohm, et al. 2009; Knudsen et al., 1987; Buneo and Andersen, 2006). However, reference frame transformations can induce noise that depends on the amount of transformation required (van Beers et al., 2002; Soechting and Flanders, 1989). Here we investigate whether the perceptual system is affected by noise in reference frame conversions.

Previous studies have analyzed the precision of visual and proprioceptive position estimates in a position matching task (van Beers et al. 1998; Clark et al. 1995). They found that the precision of vision was in the range of 0.2 +/- 0.6 (degrees of visual angle) for visual localization while the precision for proprioceptive localization for the elbow and shoulder joints combined was between 0.6 to 1.1 degrees, with the shoulder joint being more precise than the elbow (van Beers et al. 1998, Scott and Loeb, 1994; Clark et al. 1995). The estimate of proprioceptive position sense was more precise when subjects judged fingertip position rather than joint angles (Fuentes and Bastian, 2010; van Beers et al., 1998). It is unknown whether these estimates are invariants of our sensory systems or whether they depend on the task context.

By incorporating both visual and proprioceptive perception, our experiment set out to determine how context – such as extraretinal head roll signals – affects the ability to perceive the environment. This study was motivated by recent findings suggesting that reference frame transformations add noise to the transformed signal (Sober and Sabes, 2003) and that this noise might depend on the amplitude of the required transformation (Blohm and Crawford, 2007; Burns and Blohm, SfN 2009). If this was true, then changing the transformation amplitude in the coordinate matching transformation required for perception should affect the perceptual thresholds.

To test this hypothesis, head roll was introduced into a situation where a visual target position was compared to the proprioceptive localization of the fingertip. In order to compare the positions of both the target and hand location these representations needed to be converted in to a common frame of reference, so that a spatial relationship between these parameters could be formed (Soechting and Flanders, 1992). We predicted that head-roll-dependent noise increasing either of the sensory signals (vision or proprioception) should affect the precision of perceptual comparison between hand and target. We demonstrate that this was true in our data and discuss how this affects our understanding of brain function.

4.3 Materials and Methods

4.3.1 Participants

Seven subjects between the ages of 23 and 26 (3 women) participated in this study. They all had normal or corrected to normal vision and performed a reaching task with their dominant right hand. All of the participants provided written informed consent to the experimental conditions that were approved by the Queen's University General Board of Ethics.

4.3.2 Apparatus

Subjects performed this experiment using a robotic exoskeleton, (KINARM, BKIN Technologies, Kingston, Ontario, Canada) that allows both flexion and extension at the shoulder and elbow joints. The KINARM, which restricts movements to the horizontal plane, can record kinematic information of the joints, as well as apply independent mechanical loads to the shoulder and/or elbow. Participants' heads were securely positioned using a mounted bite bar that could be adjusted vertically up or down), tilted forward and backward (head pitch), and rotated left or right (head roll). An overhead projector and semitransparent mirror were used to display visual feedback of both targets and hand positions. Visual information about hand position was occluded by an opaque screen, but could be displayed through the use of a representative visual target.

4.3.3 Task Design

Subjects actively aligned their right pointer fingertip; represented by a 1cm white diameter circle; to the starting position. The start position was represented by a crosshair (2 cm tall/wide) that was located 40 cm straight-ahead of the body, midline between the shoulders. When the hand was within 4cm of the starting crosshair, a visual cue representing the right fingertip was displayed and subjects had to align the fingertip with the cross. After 500 milliseconds the right hand was passively moved by the KINARM from the start position to the central point of our target grid display, neither of which was visually displayed (Figure 13). For each trial, the fingertip could be positioned anywhere within a 6cm radial invisible circle, located 11cm in front of the cross hair and the right fingertip was held there until the end of the trial. After 250ms a visual target (1.0cm white dot) appeared for 500ms at a target position that was randomly sampled within a list of possible target locations. The target grid display making up all possible target locations was composed of four quadrants surrounding current fingertip position (see Figure 13). Within each of these four quadrants were sixteen target positions, located at 1, 3, 6 and 10 cm intervals on both the x and y axis (see Figure 13). The number of times each target was displayed throughout each block is represented by the numbers within the black target circles in Figure 13, totaling 116 trials per block. Upon trial completion subjects were required to respond with their left hand, which was

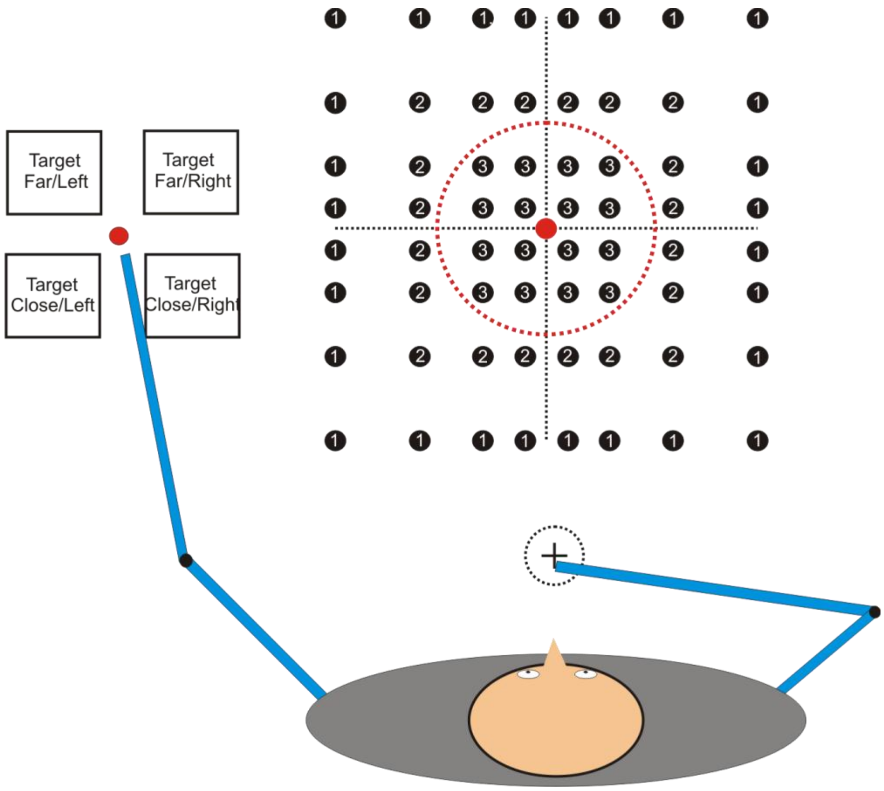

Figure 13: Experimental display.
Subjects began each trial by aligning their finger to the cross that was aligned to the midline of the body. The right hand was represented by a visual target only when it was within the dotted circle (4cm diameter) surrounding the cross at the beginning of each trial. Subjects arm (blue rectangles on right) was then passively moved by the KINARM to a location within the red dotted circle (12 cm diameter). The center of the target display, (solid red circle in the center of the four quadrants) would move to align with the fingertip position. For each trial one of the targets (black circles) within one of the four quadrants would appear. The numbers within each target represent the number of times throughout the block that that target would appear at that position. To the left of the target display, four response boxes (black outlines boxes) were positioned. Subjects would make a response indicating what location the target appeared relative to the hand by moving with their left hand to the associated response box. Text within these boxes is for schematic purposes and did not appear during testing.

passively held at the center of the virtual response box (Figure 13, left side) throughout the experiment. Subjects performed a 4-alternative forced choice task and had to judge which quadrant the target appeared relative to their right fingertip. For example, if the target appeared up and to the right of their right fingertip, then they would respond by moving their left pointer fingertip to the response box that was up and to the right of their left fingertip (Figure 13). Subjects were required to respond within 2 seconds of visual target presentation, after which four audio beeps signaled to respond. If subjects still failed to respond, the trial was aborted and marked as a bad trial.

Subjects completed this task at three different head roll orientations, i.e. -30 deg (towards left shoulder), 0 deg and 30 deg (towards right shoulder). Head orientations were randomized for each block (but fixed within a block), with subjects completing a total of 12 blocks (4 blocks per head roll condition). Subjects completed 464 trials for each head roll conditions, totaling 1392 trials.

4.3.4 Rationale

Figure 14 lays out the concept of our hypothesis and the expected effect on the data. For each trial in our experiment there was a set distance between the visual target and the unseen hand position. Subjects needed to determine where the hand was relative to the fingertip location. To do this, subjects localized the target and the fingertip and made a judgment about the distance between them. Figure 14A illustrates how head orientation affects the transformation of visual and proprioceptive information when combining into a common frame of reference. Figure 14B represents a probability distribution of the judgment for an example hand-target distance. On average, the

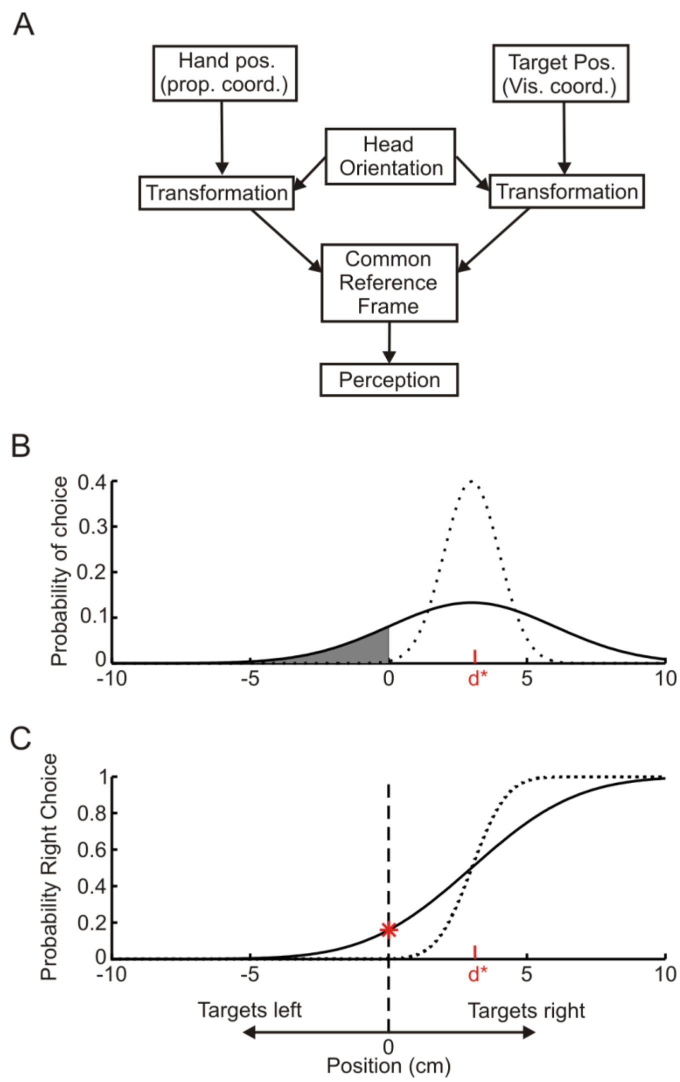

Figure 14: Hypothesis rational
(A) Schematic of head roll influencing coordinate transformations. **(B)** Probability distributions for the perception of distance (d*) between the hand and target position for normal (dotted line) and noisy (solid line) sensory conditions. **(C)** Psychometric functions representing normal dotted line) and noisy (solid line) sensory conditions. The Y axis represents performance in terms of the percentage that subjects indicated that the hand was to the right of the target. This is plotted for actual target positions that appear to the left (0 to -10) and to the right (0 to 10) of the hand.

judgment will be “positive distance”, i.e. right, (around 3cm in this example); however, random draws from the distribution will sometimes result in a “negative distance” judgment (left). The percentage of “right” judgments is then the performance at a certain hand-target distance.

The probability density functions in Figure 14B change when noise is added to the incoming sensory information (e.g. dotted line: lower noise; solid line: higher noise). We hypothesize that when the head is rolled, the distribution becomes wider because of added head-roll-dependent noise leading to higher uncertainty about the real hand-target distance and therefore there are more possible distances that could be chosen (solid line). Now, there is a possibility that subjects could choose the hand to be to the left of the target when it is actually right (shaded area), thus incorrectly identifying the position of the hand relative to the target.

Figure 14B represents the differences that occur in performance when noise is added to the sensory systems. The total percentage of right choices (shaded area in Figure 14B) for a certain hand-target distance corresponds to one point on the psychometric function in Figure 14C. The actual distance (d*) of the target is displayed along the x axis. More noise in the signals used by the perceptual system thus translates in wider probability density functions, which results in shallower psychometric functions. Therefore, using a psychometric function displaying the percentage of right responses (hand is right of target) illustrates the response differences between normal and noisy conditions. We used the slope of the psychometric function to assess whether head-roll-dependent noise influenced the perception of hand-target distance.

4.3.5 Data Analysis

Angular positions of the shoulder and elbow joints were sampled at a rate of 1000Hz, and were low-pass filtered (25 Hz, two-pass, sixth-order Butterworth). Offline analyses were performed in MATLAB (The Mathworks, Natick, MA). We ran a psychometric function fit algorithm (Wichmannand Hill, 2001a; 2001b) using a bootstrap method to assess positional biases and variances between the 3 different head roll conditions. In order to obtain this data, the 4-alternative forced-choice responses were fitted to a standard psychometric function. Using the aforementioned bootstrap method, 900 iterations were run on the data, where threshold and slope were examined at 0.5(50%) performance (Wichmann and Hill, 2001a; 2001b). The x (right-left) and y (close-far) data was compressed in order to separately view how head roll affected perception in both of these directions. For example, to analyze the left-right effect all of the data that corresponds to each target position in x (+/- 1, 3, 6, 10 cm) is merged into one group across all y positions. We were most interested in the slope and threshold at the 50% performance point. This represents the transition period where the subject’s perception of the target position relative to the hand shifted from left of the fingertip to the right, or from closer to further. This analysis allowed us to compare the slopes and view any transition biases between head roll conditions

4.4 Results

A total of 8352 trials were analyzed, with 114 trials being excluded because subjects did not respond. The goal of this experiment was to determine the accuracy to which subjects could perceive the position of their fingertip in space. This task required subject to indicate if they perceived whether the dot was to the right or left of the fingertip, as well as if it was close or far. Thus we were able to analyze the perceptual ability in both x and y directions.

Using a psychometric function, we plotted the percent of performance against the target distance, for left-right and close-far axes. Performance data is plotted for the left-right direction (Figure 15A), for each head roll position (red -30deg, blue 0deg, green 30deg). This graph represents subject's performance based on the subjects responding that the target was to the right of their fingertip. The x axis displays the distances that the target appears relative to the fingertip (negative is to the left). When the target appeared 10cm to the right of the fingertip, 100% of the time subjects reported that the target was right of the fingertip. As the targets appeared closer to the fingertip, the percentage of right responses decreased. When performance reached chance (50%), subjects began viewing the target as being to the left of the fingertip. The transition period occurred to the left (negative x-values), suggesting that subjects in general had a slight bias in estimating the location of their unseen finger tip.

Figure 15B displays the hand-target distance at which the transition for each of the head roll conditions occurred (perceptual threshold) as a function of head roll angle. An ANOVA revealed that there was a significant difference in threshold between all three head roll conditions ($F(6)=42181.54$, $p<0.01$). More specifically a t-test revealed that there was a significant difference of thresholds between the 30deg and 0deg head roll conditions ($t(6)=4735$, $p<0.01$) as well as between the -30deg and 0deg head roll conditions ($t(6)= 937.14$, $p<0.01$). With the threshold of the 0deg head roll condition falling between the thresholds of the -30deg and 30deg head roll conditions, this findings suggest that head roll created a bias in the perception of fingertip location. For instance,

X Plots

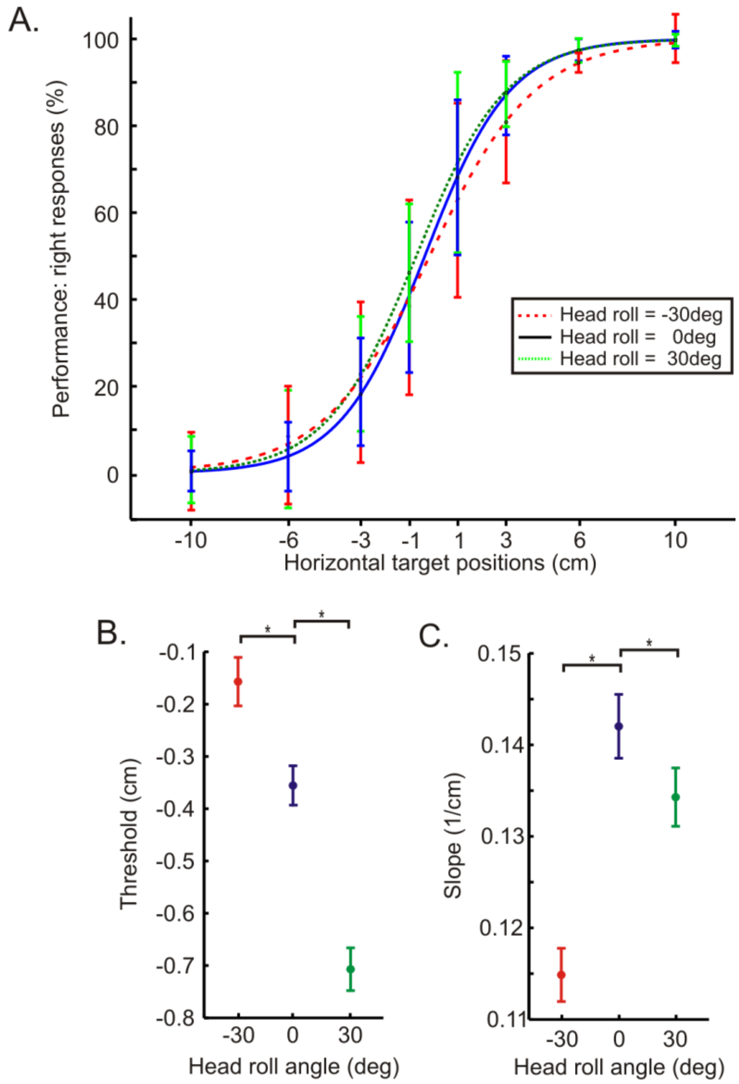

Figure 15: Performance, threshold and slope for x-data
(A) Psychometric functions representing all left-right performance data. This panel shows the percentage of right responses (y-axis) for each target position (x-axis), under all three head roll conditions: -30deg (red), 0deg (blue), 30deg (green). **(B)** Thresholds (i.e. x-axis values at chance performance) are shown for each head roll angle (-30deg, 0deg, 30deg). **(C)** Slopes from the psychometric function at 50% performance are represented for each head roll angle (-30deg, 0deg, 30deg).

when the head was tilted 30 degrees to the right shoulder, subjects perceived the targets as being more to the right of their fingertip, than when the head was straight. The same bias occurred for the -30deg head roll condition, but in the opposite direction.

Figure 15C represents the slope of the psychometric function at chance performance for each head roll condition. As explained in the Methods section, the slope is an indicator of the noisiness in the sensory signals underlying the perceptual decision. The results show a significant difference between all three head roll conditions ($F(6)= 15376.82$, $p<0.01$), with significant between 0deg and -30deg head roll conditions ($t(6)936.92$, $p <0.01$), as well as between the 0deg and 30 deg head roll conditions ($t(6)= 598.01$, $p<0.01$). When the head remained upright (0 deg head roll), the slope was largest, which was indicative of a better perceptual discrimination of the hand-target distance.

In addition to looking at the effect of head roll on perception along the left-right axis, we also analyzed the psychometric function representing performance for the data in the close-far direction (Figure 16A). Here, the x axis represents the target positions closer or further in space relative to the fingertip location, with positive values representing spatial locations further away from the fingertip. Each head roll position (red -30deg, blue 0deg, green 30deg) is plotted as a function of performance based on the subjects responding that the visual cue appeared further away from the fingertip. When the target appeared 10cm further or closer than the fingertip, subjects reported with 100% accuracy. As the targets moved closer to the fingertip, the perceptual performance decreased.

Y Plots

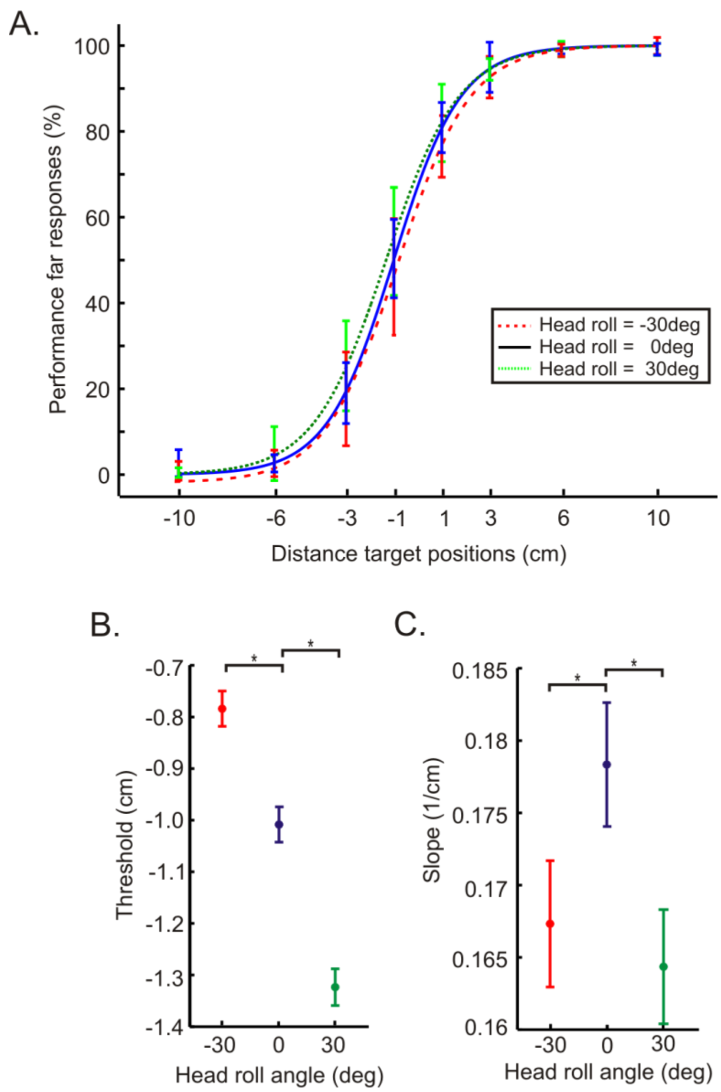

Figure 16: Performance, threshold and slope for y-data
Performance along the close-far axis. Same representation as in Figure 3. (A) Psychometric functions for all head rolls. (B) Thresholds. (C) Slopes. Error bars represent standard deviation.

Threshold measures were also computed for data in the close-far direction (Figure 16B). Significant differences in thresholds were found between all three head roll conditions with ($F(6) = 59510.43$, $p<0.01$). Where the head straight (0deg) and -30deg head roll conditions were significantly different ($t(6) = 2418$, $p<0.01$); as well as head straight and 30 deg head roll conditions ($t(6)=1465.7$, $p<0.05$). In general subjects tended to have a slight bias for perceiving visual stimuli as being further away from the hand (negative thresholds). With the threshold for the 0deg head roll condition falling in between the 2 eccentric head roll conditions (30deg and -30deg), this suggests that changing head roll orientation affected subjects' ability to perceive the location of visual stimuli with respect to their fingertip. When the head was rolled to the right, subjects were more likely to perceive targets being further away from the fingertip than when the head was rolled toward the left shoulder.

In addition to thresholds, we also analyzed the slopes for each head roll condition for data in the close-far direction finding significant differences between all orientations ($F(6)$ 2656.36, $p<0.01$). The head straight condition (0deg head roll) had a significantly larger slope than the -30deg head roll ($t(6)=1084$; $p< 0.01$) and 30deg head roll ($t(6)=1464.2$, $p<0.01$) conditions (Figure 16C). This suggests that when the head was straight, subjects had a greater ability of telling the difference of when targets appeared further or closer to the fingertip.

4.5 Discussion

This study showed that the localization of proprioceptive hand position relative to a visual target can be affected by head roll. We found significant differences in threshold and slope between head straight and head roll conditions, with head roll inducing systematic biases in perception. We suggest that head-roll induced signal-dependant noise could account for these findings; we propose that as the head moves away from an upright position additional noise is added to the sensory system resulting in less accurate perceptual discriminations of hand-target distance.

When we changed the position of head orientation to roll toward the left or right shoulder (-30 or 30 deg), we found that our perception of the location of the visual stimuli relative to our hand position changed. Significant differences in threshold values were found between each head roll condition in both the left-right and close-far directions. This indicates that seemingly unrelated, contextual variables – such as head roll – can bias perception. Similar affects of head rotation on perception were published in a study analyzing the affect of neck afferents on subjective orientation (Guerraz et al., 2000). They found that when the head was tilted at angles up to 35 degrees, the subjective visual vertical was displaced toward the direction of the head tilt (Guerraz et al., 2000).

The second effect of head roll was the distinction in slope values between head straight and head rolled conditions for both left-right and close-far directions. Head straight conditions displayed significantly larger slope values compared to both -30 and 30 head roll conditions. A larger slope value indicates a steeper transition in the psychometric curve. Thus the ability to distinguish the target appearing either to the left or the right of the hand is better during the head straight conditions. Tarnutzer and colleagues studied the effect of head roll during whole body rotation on verticality perception, finding that the most accurate performance occurred when the head was upright (Tarnutzer et al., 2010, Tarnutzer et al., 2009). Their results are indicative of larger noise associated with eccentric head roll orientations, which is in agreement with our hypothesis. Our data thus provides evidence for signal-dependent noise in the coordinate matching transformations underlying perception.

The differences observed for rolled head orientation could be explained by signal-dependant head roll noise (Van Beuzekom and Van Gisbergen, 2000; Wade and Curthoys 1997; Blohm and Crawford, 2007). This noise may be coming from the vestibular system, or muscle spindles in the neck signaling head orientation (Lechner-Steineitner, 1978; Sadeghi et al., 2007; Faisal et al., 2008; Scott and Loeb 1994; Guerraz et al., 2000). Any noise added to the signal could thus affect any transformations that need to occur in the system (Sober and Sabes, 2003, 2005). Although we don’t know how these transformations happen, we have previously shown that head roll noise can affect reference frame transformations in a reaching task (Burns and Blohm, SfN 2009).

This finding has implications in various aspects of motor control and sensorimotor research. Our results show that changes in body geometry can affect how we perceive our environment by making perception less precise. Could there be a behavioral gain from this strategy? It appears that being less precise also translates into being more fault-tolerant. For example, feeling (proprioception) and seeing the hand at the same time with both signals indicating different positions with high reliability, then we might actually perceive the viewed hand as not being ours, because there is a sensory conflict. Therefore, in unusual or more complicated geometrical arrangement of the body, it is advantageous to be less precise but more fault-tolerant and thus avoid perceived sensory conflict.

Chapter 5

General Discussion

The goal of this research was to explore the influence of head roll on multi-sensory integration. We suggest that head roll increases the amount of noise within the system, and that this additional noise should affect our perception, as well as multi-sensory weighting. For our first experiment we used a reaching task to investigate the effect of signal-dependant noise on multi-sensory weighting. To test for this, we introduced not only changes in head roll, but also we created conflict between viewed and actual hand position. Measuring reach errors provoked by these sensory conflicts allowed us to analyze how subjects weighted visual and proprioceptive information. By introducing changes in head roll position; we could compare the reach output for all three head roll conditions to determine if changing head orientation influences multi-sensory integration. Our data confirmed that head roll not only affects reach error but variability as well. With significant differences in variability between head straight and head rolled conditions we suggest that the associated signal-dependent noise would affect sensory weighting. To demonstrate this quantitatively, we created a model for multi-sensory integration and reference frame transformations. The output of this model displayed significant differences in sensory cue (vision and proprioceptive) weighting when the head was rolled. The result of this experiment suggests that the brain has knowledge of the uncertainty that is associated with sensory cues, and it can adjust the weights accordingly.

For the first experiment we wanted to know how head roll would affect action, but for the second experiment we wanted to assess how it could affect our perception. Subjects performed a task where they judged the position of their fingertip relative to a visual target. Using a psychometric function to represent the data, we plotted the performance of right or far responses against the target locations, in both x and y directions. At 50% performance, we calculated both slope and threshold, finding significant differences between head straight and rolled conditions for both parameters. These results suggest that more noise is added to the sensory system as the head moves away from an upright position, suggesting that changes in body geometry can affect how we perceive our environment by making perception less precise, and thus influence multi-sensory integration.

Limitations

1. The model that we developed to explain our findings was based in 2D space, where as everyday interactions occur in a 3D environment. The transformations that have been explained are based on x and y coordinates, not taking into account changes in the vertical direction (z). The exclusion of this third dimension can limit the implications that our model can have within 3D space.
2. Our results suggest that head roll introduces signal-dependant noise. We propose two main sources of signal-dependant noise (muscle spindles within the neck and/or the vestibular system); however it is unclear to what degree each contributes.
3. Finally, the differences in head roll conditions could be the result of subjects simply not being exposed enough to these geometrical configurations. The ability to

differentiate if noise or simply a lack of exposure to this specific postural position is the cause of our results is unknown.

Future directions

1. The present experiments open several possibilities for future research in multi-sensory integration tasks. As just mentioned the results of this experiment could be due to subjects simply not being subjected to living in a world with their head tilted. Perhaps exposing subjects to more time in these positions would allow them to learn how to more accurately judge their position sense and to interact more effectively with that environment.

2. Another possible experiment continuing this research could try to determine the contributions of both the muscle spindles within the neck and the vestibular system. One possible way to test this is to load a statically positioned head in roll with weight, therefore increasing the amount of muscle spindle activity, and in theory the amount of sensory related noise. A second option would be to knock out the vestibular system by shooting cold water into the ear, thus reducing the activity of the vestibular nerve. If perhaps the influence of head roll was altered in either of these situations it would give insight into the variables that contribute to extra sensory noise.

3. It would also be relevant to conduct an imaging study to determine how activity changes in the brain when head roll is induced during a perceptual task.

Summary

These experiments together demonstrate that introducing extraretinal signals, such as head roll, not only affect our perception but influence the way our brains weight and integrate visual and proprioceptive information. We suggest that head-roll induced signal dependant noise could account for these findings. We developed a model to explain how signal-dependant noise could affect reference frame transformations. In this model, reference frame transformations occur at a cost, which translates into added noise (i.e. variability) in the sensory signals being transformed. Because the brain adjusts these sensory weights according to the reliability of the individual sensory representations (including the transformation noise), this suggests that the brain has online knowledge about the uncertainty associated with the internal representations. In essence, multisensory weights are not set in stone and can be adapted to the context.

Appendix A

Bayesian multi-sensory integration model

In the following sections, we describe the mathematical details of our model. We will assume that all sensory variables to have a certain estimate μ with Gaussian associated noise σ^2. Joint angles will be denoted by θ whereas Euclidean variables are x. Vectors **x** are bold, matrices A are capitalized.

Forward/inverse kinematics

Figure 3B shows the arrangement of the body in the experimental setup with the hand at the IHP location. Since in our case the forearm was approximately parallel to the work surface (right panel of Figure 3B), we can fully characterize the spatial arm position **x** as a function of two joint angles $\boldsymbol{\theta}$, i.e. deviation from straight-ahead (θ_1) and upper arm elevation (θ_2):

$$x_1 = -\sin\theta_1 \cdot (\mathrm{L}_1 \sin\theta_2 + L_2) \qquad \text{Eq. 1}$$

$$x_2 = \cos\theta_1 \cdot (\mathrm{L}_1 \sin\theta_2 + L_2) \qquad \text{Eq. 2}$$

where $L_{1/2}$ are the upper arm and forearm lengths respectively. In order to compute the *inverse kinematic* transformation of the noise covariance matrix, we used a first-order Taylor expansion of $\mathbf{x}(\boldsymbol{\theta})$ around current joint angles $\boldsymbol{\theta}^0$, i.e. $\boldsymbol{x_k}(\boldsymbol{\theta}) \cong \boldsymbol{x_k}(\boldsymbol{\theta}^0) + \sum_i \frac{\partial \boldsymbol{x}_k}{\partial \boldsymbol{\theta}_i}\Big|_{\boldsymbol{\theta}^0} (\boldsymbol{\theta}_i - \boldsymbol{\theta}_i^0)$. **x** can then be written as a linear combination of $\boldsymbol{\theta}$, i.e. $\boldsymbol{x} = A\boldsymbol{\theta} + \boldsymbol{b}$, with

$$A = A(\boldsymbol{\theta}^0) = \begin{pmatrix} -\cos\theta_1^0 \cdot (L_1 \sin\theta_2^0 + L_2) & -L_1 \sin\theta_1^0 \cos\theta_2^0 \\ -\sin\theta_1^0 \cdot (L_1 \sin\theta_2^0 + L_2) & L_1 \cos\theta_1^0 \cos\theta_2^0 \end{pmatrix} \qquad \text{Eq. 3}$$

This allows us to write the covariance matrix Σ of **x** as a function of the covariance matrix of $\boldsymbol{\theta}$, as:

$$\Sigma_{\mathbf{x}} = \mathrm{A}(\boldsymbol{\theta}^0)\Sigma_{\boldsymbol{\theta}}\mathrm{A}(\boldsymbol{\theta}^0)^{\mathrm{T}} \qquad \text{Eq. 4}$$

The same approach can be used to compute the *forward kinematics* with

$$\theta_1 = \tan^{-1}\left(-\frac{x_1}{x_2}\right) \qquad \text{Eq. 5}$$

$$\theta_2 = \sin^{-1}\left(\frac{\sqrt{x_1^2+x_2^2}-L_2}{L_1}\right) \qquad \text{Eq. 6}$$

$$\text{and } A = A(\boldsymbol{x}^0) = \begin{pmatrix} -\frac{x_2^0}{{x_1^0}^2+{x_2^0}^2} & \frac{x_1^0}{{x_1^0}^2+{x_2^0}^2} \\ \frac{x_1^0}{L_1\cdot\sqrt{{x_1^0}^2+{x_2^0}^2}}\cdot c & \frac{x_2^0}{L_1\cdot\sqrt{{x_1^0}^2+{x_2^0}^2}}\cdot c \end{pmatrix} \qquad \text{Eq. 7}$$

$$\text{with } c = \sqrt{1-\left(\frac{\sqrt{{x_1^0}^2+{x_2^0}^2}-L_2}{L_1}\right)^2} \qquad \text{Eq. 8}$$

$$\text{Then, } \Sigma_{\boldsymbol{\theta}} = \mathrm{A}(\boldsymbol{x}^0)\,\Sigma_{\mathbf{x}}\mathrm{A}(\boldsymbol{x}^0)^{\mathrm{T}} \qquad \text{Eq. 9}$$

Reference frame transformation

In our case of head roll movements, the required shoulder-centered-to-retinal coordinate transformation (T) simply consists of a rotation of the angle $\theta_H=\beta H$, where β is a gain factor and H is the estimate of the head roll angle. Euclidean position in visual coordinates ($\mathbf{x}_V$) can thus be obtained from Euclidean position in proprioceptive coordinates ($\mathbf{x}_P$) using $\mathbf{x}_V=\mathrm{T}\mathbf{x}_P$ with

$$T = \begin{pmatrix} \cos\theta_H & \sin\theta_H \\ -\sin\theta_H & \cos\theta_H \end{pmatrix} \qquad \text{Eq. 10}$$

Since head roll (H) and thus θ_H are noisy variables, the transformation T introduces new noise on top of rotating the proprioceptive (P) covariance matrix into visual coordinates (V). We designed this new noise to be composed of a constant component σ_T^2 simulating the fact that all transformations have a cost (Sober and Sabes, 2003) and a head orientation signal-dependent component Σ_H.

$$\Sigma_{\mathrm{V}} = \mathrm{T}\,\Sigma_{\mathrm{P}}\mathrm{T}^{\mathrm{T}} + \sigma_{\mathrm{T}}^2 I + \Sigma_{\mathrm{H}} \qquad \text{Eq. 11}$$

From random matrix theory we know that any matrix can be decomposed into a constant and variable component, such that $A=A_0+E$, where A_0 has zero variance and E zero mean. Then, perturbation theory tells us that any linear transformation of a noisy variable $\mathbf{x}=\mathbf{x}_0+\mathbf{e}$ can be written $\mathbf{y}=A\mathbf{x}=(A_0+E)(\mathbf{x}_0+\mathbf{e})=A_0\mathbf{x}_0+A_0\mathbf{e}+E\mathbf{x}_0+E\mathbf{e}$. The covariance of $\mathbf{y}$ can then be approximated by the covariance of $A_0\mathbf{e}+E\mathbf{x}_0$, since the covariance of $E\mathbf{e}$ is negligible and $A_0\mathbf{x}_0$ has zero covariance. Thus $\Sigma_y=A_0\Sigma_x A_0^T+\Sigma_E$. In our case, the matrix Σ_E represents the variability resulting from the fact that the angle of the reference frame transformation is variable. This results in variability added to the direction orthogonal of $\mathbf{y}$. Representing $\mathbf{y}$ in polar coordinates $\boldsymbol{y} = r \cdot \begin{pmatrix} cos\theta_y \\ sin\theta_y \end{pmatrix}$ results in:

$$\Sigma_{\mathrm{H,ij}} = r|H|\sigma_H^2 \left(\frac{\partial y_i}{\partial \theta_y}\right)\left(\frac{\partial y_j}{\partial \theta_y}\right) = r|H|\sigma_H^2 \begin{pmatrix} \sin^2\theta_y & cos\,\theta_y\,sin\,\theta_y \\ cos\,\theta_y\,sin\,\theta_y & \cos^2\theta_y \end{pmatrix} \qquad \text{Eq. 12}$$

Note that, as expected, this term introduces errors perpendicular to the rotated vector. The reason for this is that variability in the rotation leads to noise only in the rotational direction around the transformed vector $\mathbf{y}$.

The inverse transformation and associated covariance matrix can simply be computed by replacing the head roll angle H by –H.

Multi-sensory integration

At the heart of the model is the multi-sensory integration step that combines proprioceptive and visual sensory information. In our model (Figure 3A), this integration occurs twice, once in visual coordinates as part of computing the visual desired movement vector and once in proprioceptive coordinates, which is required to transform the desired movement vector into a change in joint angles when determining the motor command. From basic multivariate Gaussian statistics, the means $\boldsymbol{\mu}$ and covariances Σ of the combined IHP estimates from vision (V) and proprioception (P) writes as:

$$\Sigma = \left(\Sigma_P^{-1} + \Sigma_V^{-1}\right)^{-1} \qquad \text{Eq 13}$$

$$\boldsymbol{\mu} = \Sigma \cdot \Sigma_{\mathrm{P}}^{-1}\boldsymbol{\mu}_{\mathrm{P}} + \Sigma \cdot \Sigma_{\mathrm{V}}^{-1}\boldsymbol{\mu}_{\mathrm{V}} \qquad \text{Eq. 14}$$

As mentioned above, this calculation is carried out twice, once in proprioceptive and once in visual coordinates. In visual coordinates, the sensory Euclidean visual information is combined with the transformed (forward kinematics and reference frame transformation) proprioceptive information (Euclidean). In proprioceptive coordinates, the sensory proprioceptive joint angles are combined with the visual information transformed into joint coordinates (inverse reference frame transformation and inverse kinematics).

To recover the weight matrix of the visual IHP estimate, we used $\Sigma \cdot \Sigma_{\mathrm{V}}^{-1} = \alpha$ and $\Sigma \cdot \Sigma_{\mathrm{P}}^{-1} = 1 - \alpha$ to follow (from subtraction of one from the other) that $\alpha = \frac{1}{2}\left(\Sigma \cdot \Sigma_{\mathrm{V}}^{-1} - \Sigma \cdot \Sigma_{\mathrm{P}}^{-1} + I\right)$, where I is the identity matrix.

Final motor command

Once the IHP estimate from the previous step has been subtracted from the target location ($\Delta\mathbf{x}=\mathbf{tar}-\boldsymbol{\mu}$, $\sigma_{\Delta x}^{2}=\sigma_{\mu}^{2}+\sigma_{tar}^{2}$), the resulting desired movement vector $\Delta\mathbf{x}$ needs to be transformed into a motor command $\dot{\boldsymbol{x}}$. Here, we used a previously described velocity command model (Sober and Sabes, 2003; 2005) to perform this step as follows:

$$\dot{\boldsymbol{x}} = J(\boldsymbol{\theta})J^{-1}(\widehat{\boldsymbol{\theta}})\,\Delta\,\boldsymbol{x} \qquad \text{Eq. 15}$$

Where J is the Jacobian of the system, $\boldsymbol{\theta}$ is the actual joint configuration and $\widehat{\boldsymbol{\theta}}$ is the estimated joint configuration from the multi-sensory integration step in proprioceptive coordinates. The Jacobian matrix is defined as $J_{ik}(\boldsymbol{\theta}) = \left(\frac{\partial x_i}{\partial \theta_k}\right)$. In our case, the Jacobian and its inverse write as:

$$J(\boldsymbol{\theta}) = \begin{pmatrix} -\cos\theta_1 \cdot \left(L_1 \sin\theta_2 + L_2\right) & -L_1 \sin\theta_1 \cos\theta_2 \\ -\sin\theta_1 \cdot \left(L_1 \sin\theta_2 + L_2\right) & L_1 \cos\theta_1 \cos\theta_2 \end{pmatrix} \qquad \text{Eq. 16}$$

$$J^{-1}(\boldsymbol{\theta}) = \begin{pmatrix} \frac{-\cos\theta_1}{L_1 \sin\theta_2 + L_2} & \frac{-\sin\theta_1}{L_1 \sin\theta_2 + L_2} \\ \frac{-\sin\theta_1}{L_1 \cos\theta_2} & \frac{\cos\theta_1}{L_1 \cos\theta_2} \end{pmatrix} \qquad \text{Eq. 17}$$

To compute the covariance of the motor command, we need to propagate the variances through Eq. 15. To do so, we first re-write Eq. 15 as $\dot{\boldsymbol{x}} = J(\boldsymbol{\theta})\,\Delta\,\boldsymbol{\theta}$ with $\Delta\boldsymbol{\theta} = J^{-1}(\widehat{\boldsymbol{\theta}})\,\Delta\,\boldsymbol{x}$. Since $J(\boldsymbol{\theta})$ is a constant transformation matrix, the covariance matrix of the final motor command can be written as:

$$\Sigma_{\dot{\mathbf{x}}} = J(\boldsymbol{\theta})\,\Sigma_{\Delta\boldsymbol{\theta}}\mathrm{J}(\boldsymbol{\theta})^{\mathrm{T}} \qquad \text{Eq. 18}$$

It remains to calculate the covariance matrix $\Sigma_{\Delta\boldsymbol{\theta}}$ of the motor command expressed in joint angles. Since $J^{-1}(\widehat{\boldsymbol{\theta}})$ depends on a noisy estimate of the joint angles in proprioceptive coordinates, we again have to apply random matrix theory to approximate the noise induced by $J^{-1}(\widehat{\boldsymbol{\theta}})$, as follows:

$$\Sigma_{\Delta\boldsymbol{\theta}} = J^{-1}(\widehat{\boldsymbol{\theta}})\,\Sigma_{\Delta\boldsymbol{x}}\,J^{-1}(\widehat{\boldsymbol{\theta}})^{T} + \Sigma_{J^{-1}} \qquad \text{Eq. 19}$$

The covariance matrix $\Sigma_{J^{-1}}$ associated with the noisy inverse Jacobian is computed similar to Eq. 12 as follows (using multivariate Taylor expansion):

$$\Sigma_{J^{-1},ij} = \sum_{k,l}\left(\frac{\partial\Delta\theta_i}{\partial\widehat{\theta_k}}\right)\left(\frac{\partial\Delta\theta_j}{\partial\widehat{\theta_l}}\right)\sigma^2_{\widehat{\theta_k}\widehat{\theta_l}} \qquad \text{Eq. 20}$$

with $\frac{\partial\Delta\theta_1}{\partial\hat{\theta}_1^*} = -\frac{1}{a}\left(-sin\hat{\theta}_1^*\cdot\Delta\,x_1 + cos\hat{\theta}_1^*\cdot\Delta\,x_2\right)$

$\frac{\partial\Delta\theta_1}{\partial\hat{\theta}_1^*} = -\frac{b}{a^2}\left(cos\hat{\theta}_1^*\cdot\Delta\,x_1 + sin\hat{\theta}_1^*\cdot\Delta\,x_2\right)$

$\frac{\partial\Delta\theta_2}{\partial\hat{\theta}_1^*} = -\frac{1}{b}\left(cos\hat{\theta}_1^*\cdot\Delta\,x_1 + sin\hat{\theta}_1^*\cdot\Delta\,x_2\right)$

$\frac{\partial\Delta\theta_2}{\partial\hat{\theta}_1^*} = -\frac{L_1\sin\hat{\theta}_2^*}{b^2}\left(-sin\hat{\theta}_1^*\cdot\Delta\,x_1 + cos\hat{\theta}_1^*\cdot\Delta\,x_2\right)$

and using $a = L_1\sin\hat{\theta}_2^* + L_2$ and $b = L_1\cos\hat{\theta}_2^*$ with $\hat{\theta}_i^*$ being the predicted arm configuration after execution of the motor plan $\Delta\,\boldsymbol{x}$ (Eqs. 5, 6). Note that $\sigma^2_{\hat{\theta}_i\hat{\theta}_j}$ are the elements of the covariance matrix of $\boldsymbol{\theta}$ (from Eq. 14).

Movement direction

We were only interested in the initial movement direction. Therefore, we transformed the final motor command $\dot{\boldsymbol{x}}$ from Cartesian into Polar coordinates. To transform both the means and covariance matrix into polar coordinates, we used the following formula:

$$r = \sqrt{x_1^2 + x_2^2} \qquad \text{Eq. 21}$$

$$\tan\varphi = \frac{x_2}{x_1} \qquad \text{Eq. 22}$$

To obtain the variance or movement direction towards different targets, we rotated the covariance matrix by the angle of movement direction. For the maximum likelihood estimation (MLE) procedure described below, we then only used $\Sigma_{(\mathrm{r},\phi),22}$, i.e. the variance orthogonal to the movement angle, and transformed it into angular units.

Model fitting: maximum likelihood estimation (MLE)

To estimate the model parameters from the data, we used a standard maximum likelihood estimation procedure. To do so, we calculated the negative log-likelihood (*L*) for our data to fit the above model given the set of fitting parameters ρ:

$$L_\rho(\mu, \sigma^2|\boldsymbol{y}) = -\frac{n}{2}\ln(2\pi) - \frac{n}{2}\ln(\sigma^2) - \frac{1}{2\sigma^2}\sum_i (y_i - \mu)^2 \qquad \text{Eq. 23}$$

where (μ, σ^2) are the mean and variance resulting from the model given the parameter set ρ, *n* is the number of data points and **y** contains the data measured from the experiment. We can then search for the maximum likelihood estimate by minimizing L_ρ over the parameter space, as:

$$\mathrm{argmin}_\rho \, L_\rho(\mu, \sigma^2|\boldsymbol{y}) \qquad \text{Eq. 24}$$

These computations were carried out in Matlab R2007a (The Mathworks, Natick, MA, USA) using the fmincon.m (for Eq. 24) function.

To fit Sober and Sabes' (2003) original model to our data, we used a standard non-linear least-squares regression method. The model equations were the same as for the full model, but without considering variances or reference frame transformations. Visual and proprioceptive information were simply combined using scalar weights, as in Sober and Sabes (2003, 2005).

Model parameters

Upper arm and lower arm (including fist) lengths were set constant to L_1=30 cm and L_2=45 cm respectively. Shoulder location was assumed 30cm backward from the target and 25cm rightwards of the target. Forward kinematics (Eqs. 5 and 6) for the center target location directly leads to IHP joint angles of $\theta_1 = 42.5\ deg$ and $\theta_2 = -8.3\ deg$ for the deviation of straight-ahead and the upper arm elevation respectively. IHPs and target positions were taken from the experimental data.

There were 5 parameters in the model that were identified from the data, i.e. the variances of both proprioceptive (σ_P^2) joint angles (same for both) and horizontal visual (σ_V^2) IHP, the variance associated to the head roll angle (σ_H^2), a fixed reference frame transformation cost (Σ_H) and the head rotation gain for the reference frame transformation (β). The variance of target position (σ_{tar}^2) was fixed. To account for the fact that visual distance estimation is less reliable than visual angular position estimation, we set the distance variability to 2.5 * σ_V^2 (evaluated from McIntyre, Stratta and Lacquaniti 1998; Ren, Blohm and Crawford 2007; Ren et al. 2006).

The best-fit model parameters are represented in Table 1. They were obtained through bootstrapping analysis (N=100). We used a minimum number of model parameters to describe our data. In particular, we did not have two independent joint angles, as our data were not compelling enough to distinguish the effect of both.

Table 1: Model parameter fits obtained through bootstrapping analysis (N = 100): means ± SD (see Appendix 1 for details)

Parameter	**Meaning**	**Values**
σ_P^2	Proprioceptive variance	$6.44 \cdot 10^{-6} \pm 0.75 \cdot 10^{-6}$ (rad^2)
σ_V^2	Visual variance	0.347 ± 0.019 (mm^2)
σ_H^2	Head-roll-dependent variance	$2.46 \cdot 10^{-3} \pm 1.04 \cdot 10^{-3}$ (rad^2 / deg)
Σ_H	Constant transformation noise	0.297 ± 0.031 (mm^2)
β	Head roll compensation gain	1.041 ± 0.009 (.)

References

Andersen, R., and Buneo, C. (2002). Intentional maps in posterior parietal cortex. *Annual Review of Neuroscience, 25*(1), 189.

Andersen, R. A., and Mountcastle, V. B. (1983). The influence of the angle of gaze upon the excitability of the light-sensitive neurons of the posterior parietal cortex. *Journal of Neuroscience, 3*, 532.

Angelaki, D. E., McHenry, M. Q., Dickman, J. D., Newlands, S. D., and Hess, B. J. M. (1999). Computation of inertial motion: Neural strategies to resolve ambiguous otolith information. *Journal of Neuroscience, 19*(1), 316-327.

Armstrong, B., McNair, P., and Taylor, D. (2008). Head and neck position sense. *Sports Medicine, 38*(2), 101.

Baloh, R. W., and Honrubia, V. (2001). Anatomy and physiology of the vestibular system. *Clinical neurophysiology of the vestibular system* (Third ed., pp. 3). Toronto: Oxford University Press.

Batista, A. P., Buneo, C. A., Snyder, L. H., and Andersen, R. A. (1999). Reach plans in eye-centered coordinates. *Science, 285*(5425), 257-260.

Benson, A. (1982). The vestinular sensory system. In H. B. Barlow, and J. D. Mollon (Eds.), *The senses* (pp. 333). New York: Cambridge University Press.

Bergman, R. A., Afifi, A. K., and Heidger, P. M. (1999). Muscle spindle: Neural components. *Atlas of microscopic anatomy- A functional approach*.

Binder, M. D., Kroin, J. S., Moore, G. P., and Stuart, D. G. (1977). The response of golgi tendon organs to single motor unit contractions. *Journal of Physiology, 271*, 337.

Blohm, G., and Crawford, J. D. (2007). Computations for geometrically accurate visually guided reaching in 3-D space. *Journal of Vision, 7*(5)

Blohm, G., Keith, G. P., and Crawford, J. D. (2009). Decoding the cortical transformations for visually guided reaching in 3D space. *Cerebral Cortex,*

Blohm, G., Keith, G. P., and Crawford, J. D. (2009). Decoding the cortical transformations for visually guided reaching in 3D space. *Cerebral Cortex, 19*(6), 1372-1393.

Bockisch, C. J., and Haslwanter, T. (2001). 3D eye position during static roll and pitch in humans. *Vision Research, 41*(16), 2127.

Bridgeman, B. (1995). A review of the roll of efference copy in sensory and oculomotor control systems. *Biomedical Engineering,* 23, 409-422.

Buneo, C. A., Jarvis, M. R., Batista, A. P., and Andersen, R. A. (2002). Direct visuomotor transformations for reaching. *Nature, 416*, 632.

Burgess, P. R., and Clark, F. J. (1969). Characteristics of knee joint receptors in the cat. *The Journal of Physiology, 203*(2), 317-335.

Burke, D., Hagbarth, K., Lofstedt, L. (1978). Muscle spindle activity in man during shortening and lengthening contractions. *Journal of Neurophysiology*, 277, 131-142.

Burke, D., Hagbarth, K., Lofstedt, L., and Wallin, B. G. (1976). The responses of human muscle spindle endings to vibration during isometric contraction. *Journal of Physiology, 261*, 695.

Burns, J. K., and Blohm, G. (2010). Head roll influences perceived location of hand position. *40th Society for Neuroscience Conference,* San Diego, CA, USA.

Chang, S. W. C., Papadimitriou, C., and Snyder, L. H. (2009). Using a compound gain field to compute a reach plan. *Neuron, 64*(5), 744-755.

Churchland, M. M., Santhanam, G., and Shenoy, K. V. (2006) Preparatory activity in premotor and motor cortex reflects the speed of the upcoming reach. *Journal of Neurophysiology*, 96, 3130-3146.

Clark, F. J., Larwood, K. J., Davis, M. E., and Deffenbacher, K. A. (1995). A metric for assessing acuity in positioning joints and limbs. *Experimental Brain Research, 107*(1), 73-79.

Clark, F. J., and Burgess, P. R. (1975). Slowly adapting receptors in cat knee joint: Can they signal joint angle? *Journal of Neurophysiology, 38*(6), 1448-1463.

Cohen, Y. E., and Andersen, R. A. (2002). A common reference frame for movement plans in the posterior parietal cortex. *Nature Review Neuroscience, 3*, 553.

Collewijn, H., Van der Steen, J., Ferman, L., and Jansen, T. C. (1985). Human ocular counterroll: Assessment of static and dynamic properties from electromagnetic scleral coil recordings. *Experimental Brain Research, 59*(1), 185.

Collins, D. F., Refshauge, K. M., Todd, G., and Gandevia, S. C. (2005). Cutaneous receptors contribute to kinesthesia at the index finger, elbow, and knee. *Journal of Neurophysiology, 94*(3), 1699-1706.

Cordo, P. J., Flores-Viera, C., Verschueren, S. M. P., Inglis, J. T., and Gurfinkel, V. (2002). Position sensitivity of human muscle spindles: Single afferent and population representations. *Journal of Neurophysiology*, 87, 1186-1195.

Crawford, J. D., Medendorp, W. P., and Marotta, J. J. (2004). Spatial transformations for eye-hand coordination. *Journal of Neurophysiology, 92*(1), 10-19.

Crawford, J. D., and Vilis, T. (1991). Axes of eye rotation and listing's law during rotations of the head. *Journal of Neurophysiology, 65*(3), 407-423.

Deneve, S., and Pouget, A. (2004). Bayesian multisensory integration and cross-modal spatial links. *Journal of Physiology-Paris, 98*(1-3), 249-258.

Desmurget, M., Pélisson, D., Rossetti, Y., and Prablanc, C. (1998). From eye to hand: Planning goal-directed movements. *Neuroscience and Biobehavioral Reviews, 22*(6), 761-788.

Diedrichsen, J. (2007). Optimal task-dependent changes of bimanual feedback control and adaptation. *Current Biology*, 17, 1675-1679.

Duffy, C. J., and Wurtz, R. H. (1991). Sensitivity of MST neurons to optic flow stimuli. I. A continuum of response selectivity to large-field stimuli. *Journal of Neurophysiology, 65*(6), 1329-1345.

Edin, B. B., and Abbs, J. H. (1991). Finger movement responses of cutaneous mechanoreceptors in the dorsal skin of the human hand. *Journal of Neurophysiology, 65*(3), 657-670.

Edin, B. B., and Vallbo, A. B. (1990). Dynamic response of human muscle spindle afferents to stretch. *Journal of Neurophysiology, 63, 1297- 1306.*

Engel, K. C., Flanders, M., and and Soechting, J. F. (2002). Oculocentric frames of reference for limb movement. *Archives Italiennes De Biologie, 140*(3), 211.

Ernst, M. O., and Banks, M. S. (2002). Humans integrate visual and haptic information in a statistically optimal fashion. *Nature, 415*, 429.

Ernst, M. O., and Bülthoff, H. H. (2004). Merging the senses into a robust percept. *Trends in Cognitive Sciences, 8*(4), 162-169.

Faisal, A. A., Selen, L. P., and Wolpert, D. M. (2008). Noise in the nervous system. *Nature Reviews Neuroscience, 9*, 292.

Fernández, C., Goldberg, J. M., and Abend, W. K. (1972). Response to static tilts of peripheral neurons innervating otolith organs of the squirrel monkey. *Journal of Neurophysiology, 35*, 978.

Fu, Q. G., Flament, D., Coltz, J. D., and Ebner, T. J. (1995). Temporal encoding of movement kinematics in the discharge of primate primary motor and premotor neurons. *Journal of Neurophysiology, 73*(2), 836-854.

Fuentes, C. T., and Bastian, A. J. (2010). Where is your arm? variations in proprioception across space and tasks. *Journal of Neurophysiology, 103*(1), 164-171.

Gandevia, S. C., and Burke, D. (1992). Does the nervous system depend on kinesthetic informaiton to control natural limb movements? *Behavioural and Brain Sciences, 15*, 614.

Gandevia, S. C., and McCloskey, D. I. (1976). Joint sense, muscle sense and their combination as position sense, measured at the distal interphalangeal joint of the middle finger. *Journal of Physiology, 260*, 387.

Gellman, R. S., and Fletcher, W. A. (1992). Eye position signals in human saccadic processing. *Experimental Brain Research, 89*, 425.

Georgopoulos, A., Kalaska, J., Caminiti, R., and Massey, J. (1982). On the relations between the direction of two-dimensional arm movements and cell discharge in primate motor cortex. *Journal of Neuroscience, 2*(11), 1527-1537.

Ghahramani, Z., Wolpert, D. M., and Jordan, M. I. (1997). Computational models of sensorimotor integration. In P. G. Morasso, and V. Sanguineti (Eds.), *Self-organization, computational maps and motor control* (pp. 117). Amsterdam:

Gibson, J. J. (1933). Adaptation, after-effect and contrast in the perception of curved lines. *Journal of Experimental Psychology, 16*(1)

Goodale, M. A. Transforming vision into action. *Vision Research, In Press, Corrected Proof*

Goodwin, G. M., McCloskey, D. I., and Mathews, P. B. (1972). Proprioceptive illusions induced by muscle vibration: Contribution by muscle spindles to perception? *Science, 175*(28), 1328.

Goodwin, G. M., McCloskey, D. I., and Mathews, P. B. C. (1972). The contribution of muscle afferents to kinesthesis shown by vibration induced illusions of movement and by the effect of paralysing joint afferents. *Brain, 95*(4), 705-748.

Gordon, J., and Ghez, C. (1987). Trajectory control in targeted force impluses. III. compensatory adjustments for intial errors. *Experimental Brain Research, 67*, 253.

Green, A. M., and Angelaki, D. (2010). Internal models and neural computation in the vestibular system. *Experimental Brain Research, 200*(3-4), 197.

Gu, Y., Angelaki, D. E., and DeAngelis, G. C. (2008). Neural correlates of multisensory cue integration in macaque MSTd. *Nature Neuroscience, 11*, 1201.

Gu, Y., DeAngelis, G. C., and Angelaki, D. E. (2007). A functional link between area MSTd and heading perception based on vestibular signals. *Nature Neuroscience, 10*, 1038.

Guerraz, M., Luyat, M., Poquin, D., and Ohlmann, T. (2000). The role of neck afferents in subjective orientation in the visual and tactile sensory modalities. *Acta Otolaryngol, 120*, 735.

Hagura, N., Takei, T., Hirose, S., Aramaki, Y., Matsumura, M., Sadata, N., et al. (2007). Activity in the posterior parietal cortex mediates visual dominance over kinesthesia. *Journal of Neuroscience, 27*, 7047.

Hall, Z. W., and Sanes, J. R. (1993). Synaptic structure and development: The neuromuscular junction. *Cell, 72*, 99.

Harris, C. M., and Wolpert, D. M. (1998). Signal-dependent noise determines motor planning. *Nature, 394*, 780.

Haslwanter, T., Straumann, D., Hess, B. J., and and Henn, V. (1992). Static roll and pitch in the monkey: Shift and rotation of listing's plane. *Vision Research, 32*(7), 1341.

Helbig, H. B., and Ernst, M. O. (2008). Visual-haptic cue weighting is independent of modality-specific attention. *Journal of Vision, 8*(1)

Henkes, H. E., Denier van der Gon, J.J., van Marle, G. W., and Schreinemachers, H. P. (1968). Electro-oculography. A semi-automatic recording procedure. *British Journal of Ophthalmology, 52*(2), 122.

Henriques, D. Y. P., Medendorp, W. P., Khan, A. Z., and Crawford, J. D. (2002). Visuomotor transformations for eye-hand coordination. In J. Hyona, D.P. Munoz,W.Heide and R.Radach (Ed.), *Progress in brain research* (pp. 329-340) Elsevier.

Hulliger, G. (1984). The mammalian muscle spindle and its central control. *Reviews of physoilogy, biochemistry and pharmacology, volume 101* (pp. 15) Springer Berlin Heidelberg.

Jordan, M. I., Flahs, T., and and Arnon, Y. (1994). A model of the learning of arm trajectories from spatial deviations. *Journal of Cognitive Neuroscience, 6*(4), 359.

Jordan, M. I., and Rumelhart, D. E. (1992). Forward models: Supervised learning with a distal teacher. *Cognitive Science, 16*, 307.

Kalaska, J., Cohen, D., Hyde, M., and Prud'homme, M. (1989). A comparison of movement direction-related versus load direction- related activity in primate motor cortex, using a two-dimensional reaching task. *Journal of Neuroscience, 9*(6), 2080-2102.

Kawato, M., Furukawa, K., Suzuki, R. (1987). A hierarchical neural-network model for control and learning of voluntary movement. *Biology Cybernetics*, 57, 169-185.

Knill, D. C., and Pouget, A. (2004). The bayesian brain: The role of uncertainty in neural coding and computation. *Trends in Neurosciences, 27*(12), 712-719.

Knudsen, E. I., Lac, S., and Esterly, S. D. (1987). Computational maps in the brain. *Annual Review of Neuroscience, 10*(1), 41-65.

Körding, K. P., and Wolpert, D. M. (2006). Bayesian decision theory in sensorimotor control. *Trends in Cognitive Sciences, 10*(7), 319-326.

Lacquaniti, F., and Caminiti, R. (1998). Visuo-motor transformations for arm reaching. *European Journal of Neuroscience, 10*, 195.

Lechner-Steinleitner, S. (1978). Interaction of labyrinthine and somatoreceptor inputs as determinants of the subjective vertical. *Psychological Research, 40*(1), 65.

Lee, S., and Terzoloulos, D. (2006). Heads up!: Biomechanical modeling and neuromuscular control of the neck. *AMC Transactions on Graphics, 25*(3), 1188.

Leigh, R. J., and Zee, D. S. (2006). The vestibular-optokinetic system. *The neurology of eye movements* (Fourth ed., pp. 20). Toronto: Oxford University Press.

Li, W., and Matin, L. (1992). Visual direction is corrected by a hybrid extraretinal eye position signal. *Ann N Y Acad Sci., 656*, 865.

Liu, J., Thornell, L., and Pedrosa-Domellof, F. (2003). Muscle spindles in the deep muscles of the human neck: A morphological and immunocytochemical study. *Journal of Histochemistry and Cytochemistry, 51*(2), 175-186.

Ma, W. J., Beck, J. M., Latham, P. E., and Pouget, A. (2006). Bayesian inference with probabilistic population codes. *Nature Neuroscience, 9*(11), 1432.

Marg, E. (1951). Development of electro-oculography. *American Medical Association Archives of Ophthalmology, 45*, 169.

Markham, C. H. (1989). Anatomy and physiology of otolith-controlled ocular counterrolling. *Acta Oto-Laryngologica, 108*, 263-266.

Marmor, M. F., and Zrenner, E. (1993). Standard for clinical electro-oculography. *Documenta Ophthalmolgica, 85*(2), 115.

McGuire, L. M., and Sabes, P. N. (2009). Sensory transformations and the use of multiple reference frames for reach planning. *Nature Neuroscience, 12*(8), 1056.

McIntyre, J., Stratta, F., and Lacquaniti, F. (1997). Viewer-centered frame of reference for pointing to memorized targets in three-dimensional space. *Journal of Neurophysiology, 78*(3), 1601-1618.

McIntyre, J., Stratta, F., and Lacquaniti, F. (1998). Short-term memory for reaching to visual targets: Psychophysical evidence for body-centered reference frames. *Journal of Neuroscience, 18*(20), 8423-8435.

Medendorp, W. P., Goltz, H. C., Crawford, J. D., and Vilis, T. (2005). Integration of target and effector information in human posterior parietal cortex for the planning of action. *Journal of Neurophysiology, 93*(2), 954-962.

Medendorp, W. P., Goltz, H. C., Vilis, T., and Crawford, J. D. (2003). Gaze-centered updating of visual space in human parietal cortex. *Journal of Neuroscience, 23*(15), 6209-6214.

Meredith, M. A., and Stein, B. E. (1986). Visual, auditory, and somatosensory convergence on cells in superior colliculus results in multisensory integration. *Journal of Neurophysiology, 56*(3), 640-662.

Meredith, M. A., and Stein, B. E. (1986). Visual, auditory, and somatosensory convergence on cells in superior colliculus results in multisensory integration. *Journal of Neurophysiology, 56*(3), 640-662.

Miller, E. F., Fregly, A. R., and Graybiel, A. (1968). Visual horizontal-perception in relation to otolith-function. *The American Journal of Psychology, 81*(4), 488-496.

Mon-Williams, M., Wann, J. P., Jenkinson, M., and Rushton, K. (1997). Synaesthesia in the normal limb. *Proc Biol Sci., 264*(1384), 1007.

Mushiake, H., Tanatsugu, Y., and Tanji, J. (1997). Neuronal activity in the ventral part of premotor cortex during target-reach movement is modulated by direction of gaze. *Journal of Neurophysiology, 78*(1), 567-571.

Nadler, J. W., Angelaki, D. E., and DeAngelis, G. C. (2008). A neural representation of depth from motion parallax in macaque visual cortex. *Nature, 452*, 642.

Peck, D., Buxton, D. F., and Nitz, A. (1984). A comparison of spindle concentrations in large and small muscles acting in parallel combinations. *Journal of Morphology, 180*(3), 243-252.

Polit, A., and Bizzi, E. (1979). Characteristics of motor programs underlying arm movements in monkeys. *Journal of Neurophysiology, 42*(1), 183-194.

Porter, R., and Lemon, R. (1993). Corticospinal function and voluntary movement. *Monographs of the physop;pgoca; society* (). Oxford: Clarendon Press.

Proske, U., Schaible, H. G., and Schmidt, R. F. (1988). Joint receptors and kinaesthesia. *Experimental Brain Research, 72*(2), 219.

Proske, U. W. E. (2005). What is the role of muscle spindles in proprioception? *Muscle and Nerve, 31*, 780.

Purves, D., Augustine, G. J., Fitzpatrick, D., Hall, W. C., LaMantia, A., McNamara, J. O., et al (Eds.). (2008). *Neuroscience* (fourth ed.). Massachusetts: Sinauer Associates, Inc.

Ren, L., Blohm, G., and Crawford, J. D. (2007). Comparing limb proprioception and oculomotor signals during hand-guided saccades. *Experimental Brain Research, 182*, 189.

Ren, L., Khan, A. Z., Blohm, G., Henriques, D. Y. P., Sergio, L. E., and Crawford, J. D. (2006). Proprioceptive guidance of saccades in eye-hand coordination. *Journal of Neurophysiology, 96*(3), 1464-1477.

Rizzolatti, G., Fadiga, L., Gallese, V., and Fogassi, L. (1996). Premotor cotrex and the recognition of motor actions. *Cognitive Brain Research, 3*, 131.

Rizzolatti, G., Fogassi, L., and Gallese, V. (2002). Motor and cognitive functions of the ventral premotor cortex. *Current Opinion in Neurobiology, 12*(2), 149-154.

Rose, D. J., and Christina, R. W. (2006). Somatosensory contributions to action. *A multilevel approach to the study of motor control and learning* (second ed., pp. 59). Toronto: Pearson Education, Inc.

Rossetti, Y., Desmurget, M., and Prablanc, C. (1995). Vectorial coding of movement: Vision, proprioception, or both? *Journal of Neurophysiology, 74*(1), 457-463.

Sadeghi, S. G., Chacron, M. J., Taylor, M. C., and Cullen, K. E. (2007). Neural variability, detection thresholds, and information transmission in the vestibular system. *Journal of Neuroscience, 27*(4), 771.

Sainburg, R. L., Ghilardi, M. F., Poizner, H., and Ghez, C. (1995). Control of limb dynamics in normal subjects and patients without proprioception. *Journal of Neurophysiology, 73*(2), 820-835.

Sainburg, R. L., Lateiner, J. E., Latash, M. L., and Bagesteiro, L. B. (2003). Effects of altering initial position on movement direction and extent. *Journal of Neurophysiology, 89*(1), 401-415.

Sarlegna, F. R., Przybyla, A., and Sainburg, R. L. (2009). The influence of target sensory modality on motor planning may reflect errors in sensori-motor transformations. *Neuroscience, 164*(2), 597-610.

Schlicht, E. J., and Schrater, P. R. (2007). Impact of coordinate transformation uncertainty on human sensorimotor control. *Journal of Neurophysiology, 97*(6), 4203-4214.

Schone, H., and Udo De Haes, H. (1968). Perception of gravity-vertical as a function of head and trunk position. *Journal of Comparative Physiology A: Neuroethology, Sensory, Neural, and Behavioral Physiology, 60*(4), 440.

Schoultz, T. W., and Swett, J. E. (1974). Ultrastructural organization of the sensory fibers innervating the golgi tendon organ. *Anatomical Record, 179*(2), 147.

Scott, S. H. (2003). Role of primary motor cortex in goal-directed movements: Insights from neurophysioloical studies on non-human primates. *Current Opinion in Neurobiology, 13*, 671.

Scott, S. H. (2004). Optimal feedback control and the neural basis of volitional motor control. *Nature Reviews Neuroscience, 5*, 532.

Scott, S. H., Gribble, P. L., Graham, K. M. and Cabel, D. W. (2001). Dissociation between hand motion and population vectors from neural activity in motor cortex. *Nature*, 413, 161-165.

Scott, S. H., and Loeb, G. E. (1994). The computation of position-sense from spindles in mono- and multi-articular muscles. *Journal of Neuroscience, 14*, 7529.

Seidman, S. H., Telford, L., and Paige, G. D. (1995). Vertical, horizontal, and torsional eye movement responses to head roll in the aquirl monkey. *Experimental Brain Research, 105*(2), 218.

Seidman, S. H., and John Leigh, R. (1989). The human torsional vestibulo-ocular reflex during rotation about an earth-vertical axis. *Brain Research, 504*(2), 264-268.

Shadmehr, R., and Wise, S. P. (2005). *The computational neurobiology of reaching and pointing*. Cambridge: The MIT Press.

Shadmehr, W. W., S.P. (2004). Motor learning and memory for reaching and pointing. In M. S. Gazzaniga (Ed.), *The cognitive neurosciences* (3rd ed., pp. 511). Cambridge: The MIT Press.

Sober, S. J., and Sabes, P. N. (2003). Multisensory integration during motor planning. *Journal of Neuroscience, 23*(18), 6982-6992.

Sober, S. J., and Sabes, P. N. (2005). Flexible strategies for sensory integration during movement planning. *Nature Neuroscience, 8*, 490.

Soechting, J. F., and Flanders, M. (1992). Moving in three-dimensional space: Frames of reference, vectors, and coordinate systems. *Annual Review of Neuroscience, 15*(1), 167-191.

Soechting, J. F., and Flanders, M. (1989). Errors in pointing are due to approximations in sensorimotor transformations. *Journal of Neurophysiology, 62*(2), 595-608.

Stein, B. E., and Meredith, M. A. (1993). *The merging of the senses*. London: The MIT Press.

Stein, B. E., and Stanford, T. R. (2008). Multisensory integration: Current issues from the perspective of the single neuron. *Nature Reviews Neurscience, 9*, 255.

Tanaka, K., and Saito, H. (1989). Analysis of motion of the visual field by direction, expansion/contraction, and rotation cells clustered in the dorsal part of the medial superior temporal area of the macaque monkey. *Journal of Neurophysiology, 62*(3), 626-641.

Tarnutzer, A. A., Bockisch, C., Straumann, D., and Olasagasti, I. (2009). Gravity dependence of subjective visual vertical variability. *Journal of Neurophysiology, 102*(3), 1657-1671.

Tarnutzer, A. A., Bockisch, C. J., and Straumann, D. (2010). Roll-dependent modulation of the subjective visual vertical: Contributions of head- and trunk-based signals. *Journal of Neurophysiology, 103*(2), 934-941.

van Beers, R. J., Sittig, A. C., and Denier van der Gon, J.J. (1998). The precision of proprioceptive position sense. *Experimental Brain Research, 122*(4), 367.

van Beers, R. J., Baraduc, P., and Wolpert, D. M. (2002). Role of uncertainty in sensorimotor control. *Philosophical Transactions of the Royal Society of London.Series B: Biological Sciences, 357*(1424), 1137-1145.

van Beers, R. J., Haggard, P., and Wolpert, D. M. (2004). The role of execution noise in movement variability. *Journal of Neurophysiology, 91*(2), 1050-1063.

van Beers, R. J., Sittig, A. C., and Gon, J. J. D. v. d. (1999). Integration of proprioceptive and visual position-information: An experimentally supported model. *Journal of Neurophysiology, 81*(3), 1355-1364.

Van Beuzekom, A. D., and Van Gisbergen, J. A. M. (2000). Properties of the internal representation of gravity inferred from spatial-direction and body-tilt estimates. *Journal of Neurophysiology, 84*(1), 11-27.

Van Beuzekom, A. D., and Van Gisbergen, J. A. M. (2000). Properties of the internal representation of gravity inferred from spatial-direction and body-tilt estimates. *Journal of Neurophysiology, 84*(1), 11-27.

Wade, S. W., and Curthoys, I. S. (1997). The effect of ocular torsional position on perception of the roll-tilt of visual stimuli. *Vision Research, 37*(8), 1071.

Wichmann, F. A., and Hill, N. J. (2001a). The psychometric function: L. fitting, sampling and goodness-of-fit. *Perception and Psychophysics, 63*(8), 1293.

Wichmann, F. A., and Hill, N. J. (2001b). The psychometric function: Ll. bootstrap-based confidence intervals and sampling. *Perception and Psychophysics, 63*(8), 1314.

Wise, S. P., and Shadmehr, R. (2002). Motor control. In V. S. Ramachandran (Ed.), *Encylopedia of the human brain* (pp. 137). San Diego, CA: Academis Press.

Wolpert, D. M. (2007). Probabilistic models in human sensorimotor control. *Human Movement Science, 26*(4), 511-524. Wolpert, D. M., Ghahramani, z., and Jordan, M. I. (1995). An internal model for sensorimotor integration. *Science*, 269, 1880-1882.